



# Thermal-Sprayed Photocatalytic Coatings for Biocidal Applications: A Review

Yi Liu<sup>1,2</sup> · Jing Huang<sup>1,2</sup> · Xiaohua Feng<sup>1,2</sup> · Hua Li<sup>1,2</sup>

Submitted: 24 August 2020 / in revised form: 5 October 2020 / Published online: 4 November 2020  
© ASM International 2020

**Abstract** There have been ever-growing demands for disinfection of water and air in recent years. Efficient, eco-friendly, and cost-effective methods of disinfection for pathogens are vital to the health of human beings. The photocatalysis route has attracted worldwide attention due to its highly efficient oxidative capabilities and sustainable recycling, which can be used to realize the disinfection purposes without secondary pollution. Though many studies have comprehensively reviewed the work about photocatalytic disinfection, including design and fabrication of photocatalytic coatings, inactivation mechanisms, or practical applications, systematic reviews about the disinfection photocatalysis coatings from fabrication to effort for practical use are still rare. Among different ways of fabricating photocatalytic materials, thermal spray is a versatile surface coating technique and competitive in constructing large-scale functional coatings, which is a

most promising way for the future environmental purification, biomedical and life health applications. In this review, we briefly introduced various photocatalytic materials and corresponding inactivation mechanisms for virus, bacteria and fungus. We summarized the thermal-sprayed photocatalysts and their antimicrobial performances. Finally, we discussed the future perspectives of the photocatalytic disinfection coatings for potential applications. This review would shed light on the development and implementation of sustainable disinfection strategies that is applicable for extensive use for controlling pathogens in the near future.

**Keywords** coating · disinfection · inactivation mechanisms · photocatalyst · thermal spray

## Introduction

A variety of pathogens (e.g., bacteria, viruses, fungi, algae) exist in water and air (Ref 1-4). Owing to the health threat caused by infections through air, water, food and a range of other modes of infection, elimination of the pathogens is a significant concern, which leads to a growing demand for disinfection techniques (Ref 5-7). Numerous measures have been taken to tackle the microbial contamination problems, among which the conventional methods were usually based on physical and biological strategies, including conventional chemical disinfectants (e.g., chlorine, chlorine dioxide, ozone, and alcohol, formaldehyde, or hydrogen peroxide), antimicrobial drugs (e.g., antibiotics) and ultraviolet irradiation (UV-C, UV-B and UV-A) (Ref 8-11). However, the chemical disinfectants or antimicrobial drugs usually brought about other concerns including secondary toxic pollutants, drug resistance, and

---

This article is an invited paper selected from invited presentations at the International Thermal Spray Conference 2021 Virtual Preview Session on Coatings for Anti-Virus, Bacteria, and Fungus Applications, held on June 18, 2020, and has been expanded from the original oral presentation.

---

✉ Yi Liu  
liuyi@nimte.ac.cn

✉ Hua Li  
lihua@nimte.ac.cn

<sup>1</sup> Key Laboratory of Marine Materials and Related Technologies, Ningbo Institute of Materials Technology and Engineering, Chinese Academy of Sciences, Ningbo 315201, China

<sup>2</sup> Zhejiang Engineering Research Center for Biomedical Materials, Cixi Institute of Biomedical Engineering, Ningbo Institute of Materials Technology and Engineering, Chinese Academy of Sciences, Ningbo 315201, China

extra consumption (resources/energy used in producing the chemicals), while the methods using UV-induced processes have also been found to suffer from a lack of residual effect. Therefore, new disinfection techniques have been developed to address the shortcomings of the conventional methods.

Advanced oxidation processes (AOPs), including photocatalysis, offer good potential alternative for disinfection purpose without extra consumption or producing secondary pollutants. As one of the AOPs method, photocatalysis route is regarded as a most promising antimicrobial strategy. In the process of eliminating pathogens in air, water, or on solid surface, the photocatalyst can be excited by light irradiation to produce  $h^+$  and a series of powerful reactive oxide species (ROSs) including  $\cdot O_2^-$ ,  $\cdot OH$ , and  $H_2O_2$  for inactivation of pathogenic microbes without secondary pollution. There are no mass loss and performance decrease for photocatalytic materials when they perform purification functions. Therefore, photocatalysis route has a number of advantages over the conventional disinfection methods (e.g., chemical disinfectants, UV irradiation, etc.), including good reusability, long-term stability, and eco-friendliness. Since the discovery of the photocatalytic water splitting effect of  $TiO_2$  by Fujishima and Honda in 1972, research in photocatalysis has been carried out for the disinfection use, showing great potentials in air treatment, water remediation, food preservation, and many other fields (Ref 12).

Until now, photocatalytic disinfection has become an effective route for inactivation of different pathogens (e.g., bacteria, viruses, or fungi, etc.). Photocatalytic material is a key factor to achieve high effective anti-infection. In the last two decades, ever-growing efforts have been made for the development of photocatalytic disinfection applications. Two categories of photocatalysts have been developed for inactivation of microbial species: the metal oxides like photocatalysts, including  $TiO_2$  (Ref 13), zinc oxide (ZnO) (Ref 14), tungsten oxide ( $WO_3$ ) (Ref 15), and the nonmetal catalysts, such as graphitic carbon nitride ( $g-C_3N_4$ ) (Ref 16),  $C_{60}$  (Ref 17), and so on. With the advance of analytical methods for pathogens detection and increasing public health concern, there is a pressing need to evaluate the performance of photocatalysis as an eco-friendly, cost-effective, and sustainable strategy for the disinfection of air, water, and solid surface and also the future opportunities for industrial use.

Most of the photocatalytic powders and suspensions perform outstanding photocatalytic efficiency in eliminating the waterborne pathogens due to high surface area. However, drawbacks of difficulty in separation and recycling of the photocatalysts in suspension are the major factors that hindered their application in versatile environmental conditions. To tackle the problem, researchers

developed different methods to immobilize the photocatalysts onto certain solid substrates or supports, which combines the advantages of functionality and practicability in photocatalytic disinfection. Among different methods of immobilization, surface coating technique is a most promising one in fabricating functional coatings with photocatalytic antimicrobial properties.

Among different synthesis methods of surface coatings, thermal spray technique (e.g., plasma spray, flame spray, high-velocity oxygen-fuel spray, electric arc spraying, and cold spray) offers facile one-step fabrication of large-scale photocatalytic materials on arbitrary solid surfaces and also the capability of mass synthesis of photocatalytic materials via chemical reaction during the spraying processing. Therefore, the thermal spray method has great potentials in fabricating functional photocatalytic coatings with biocidal properties.

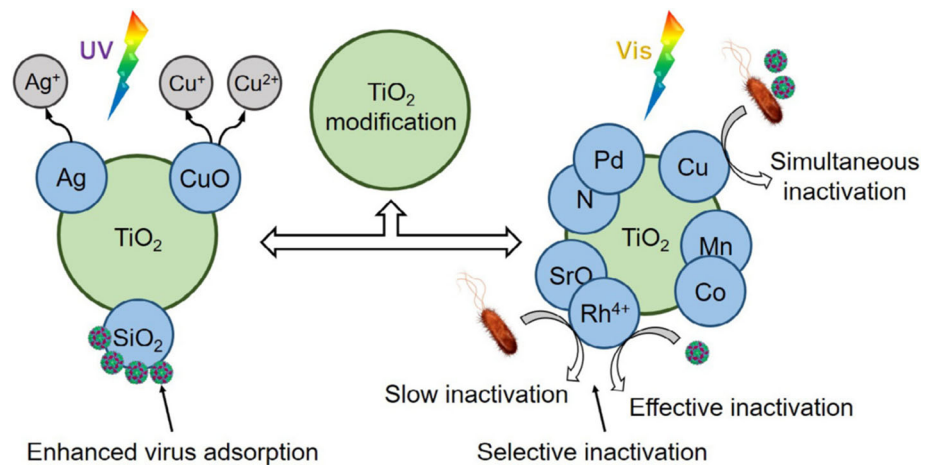
In this review, four categories of photocatalytic materials, i.e.,  $TiO_2$ - and  $TiO_2$ -based photocatalysts, metal-containing photocatalysts other than  $TiO_2$ -based materials, metal-free photocatalysts, and two-dimensional photocatalysts for pathogen inactivation, were introduced. Moreover, we critically reviewed the antimicrobial performance and mechanisms of newly developed thermal-sprayed photocatalytic coatings from different emerging trends in the last two decades. Additionally, we presented the antimicrobial mechanisms of the coatings based on generation of photoactivated reactive oxide species. Finally, we discussed the future challenges and opportunities of thermal-sprayed photocatalytic coatings in disinfection applications.

## Typical Photocatalytic Disinfection Materials

### $TiO_2$ - and $TiO_2$ -Based Photocatalysts

$TiO_2$  is one of the most widely studied photocatalysts.  $TiO_2$  was extensively explored for photocatalytic disinfection applications over the past years, which shows advantages of high photoactivity and stability, nontoxicity, and low cost. Among different types of  $TiO_2$  nanoparticles, Degussa P25 is the most popular photocatalyst, which is widely used for broad spectra anti-bacteria or anti-virus use (Ref 18, 19). Yet two major drawbacks of  $TiO_2$  nanomaterials are high recombination rates and large band gap, which limit their photocatalytic disinfection properties. Intensive efforts have been devoted to improving the photocatalytic efficiency of  $TiO_2$ . One of the most important routes is the modification of  $TiO_2$  by using metallic/nonmetallic elements or metal oxides (Fig. 1) (Ref 20–22). On the one hand, the decoration of Ag, CuO, or  $SiO_2$  nanoparticles was proved to enhance the UV-induced

**Fig. 1** Typical modifications of TiO<sub>2</sub> photocatalysts for enhanced disinfection properties (Ref 20)



bactericidal effect of TiO<sub>2</sub> photocatalysts, among which the SiO<sub>2</sub> nanoparticles were also able to enhance the virus adsorption and hence the photocatalytic inactivation efficiency. On the other hand, the decoration of metallic elements (e.g., Pd, Cu, Mn, Co), nonmetallic elements (e.g., N, F), or rare earth elements/oxides (e.g., Rh<sup>4+</sup>, SrO) were also employed to enhance the visible-induced photocatalytic inactivation effect of viruses and bacteria (Ref 23–28). Some of the recent work about modifications of TiO<sub>2</sub> photocatalysts are summarized as follows.

Precious metals like Ag and Cu are commonly used metallic elements for the TiO<sub>2</sub> modification. Younas et al. prepared Ag ion-doped TiO<sub>2</sub> nanoparticles by liquid impregnation (LI) method for antibacterial use (Ref 29). The experiments confirmed that under UV light illumination, the particles showed the disinfection efficiency of up to 16%, but when used synergistically with 1 wt.% Ag-TiO<sub>2</sub>, 100% of *Escherichia coli* (*E. coli*) bacteria were killed in 30 min. Cu is an essential trace element in living organisms; thus, it could be used as a TiO<sub>2</sub> dopant for visible-light photocatalytic activity but with less toxicity. Gladis et al. reported copper-doped TiO<sub>2</sub> nanoparticles synthesized by a two-step method. The sol–gel deposition was followed by microwave hydrothermal treatment, which achieved a band gap reduction down to 2.86 eV at a relatively low nominal doping level of 2.0% (Ref 30). Remarkable antibacterial properties against both gram-negative and gram-positive bacteria were realized by TiO<sub>2</sub>-Cu<sup>2+</sup> without any cytotoxicity to human blood cells, which was considered to be related to the leach of Cu ions in combination with the oxidative attack based on TiO<sub>2</sub> photocatalysis.

Since most metallic dopants have toxic effects, non-metallic elements (e.g., N, F), nano carbon or SiO<sub>2</sub> can be used as alternatives for modifying TiO<sub>2</sub>. By using the nonmetallic dopant, diminished toxicity and improved photocatalytic activity has been seen for the modified

catalyst. Janpetch et al. developed a hybrid nanocomposite material of bacterial cellulose (BC) nanofibers and TiO<sub>2</sub> nanoparticles, and doping of the material by nitrogen (N) and fluorine (F) gave rise to remarkably enhanced visible-light sensitivity (Ref 31). The results showed that N-F co-doped TiO<sub>2</sub> demonstrated high efficiency of photocatalytic disinfection activity against both gram-negative and gram-positive bacteria under fluorescence light. Metal and nonmetal co-doping techniques were also used to improve the photocatalytic activity of TiO<sub>2</sub>. For instance, N, W co-doping was used to narrow the band gap of TiO<sub>2</sub> to about 2.3 eV and achieve high photocatalytic activity under both UV and visible-light illumination (Ref 32).

As to carbon-modified TiO<sub>2</sub> photocatalysts, Leary and Westwood proposed several fundamental factors accounting for the enhanced photocatalytic efficiency of TiO<sub>2</sub> by incorporating carbonaceous nanomaterials, where decreased band gap, reduced charge-carrier recombination rate, and promoted adsorption of reactants on the photocatalyst surface play the predominate roles (Ref 33). Different kinds of allotropies of carbon were used for the modification of TiO<sub>2</sub>. Magnetic carbon nanotube (MCNT) composites with titanium dioxide (TiO<sub>2</sub>) have enhanced photocatalytic disinfection efficiency and better applicability than bare TiO<sub>2</sub> and/or MCNT, including better solar light applicability and easier catalyst separation process by utilizing its magnetic property. Y. Shimizu et al. investigated the bactericidal mechanism of *E. coli* by using MCNT-TiO<sub>2</sub> nanocomposites under various conditions and photocatalytic disinfection models (Ref 26). The results showed that the MCNT-TiO<sub>2</sub> composite had higher disinfection efficiencies than bare TiO<sub>2</sub>, and the physical bacterial capture was the dominant disinfection mechanism. The authors found that high disinfection rate can be realized at an optimum MCNT: TiO<sub>2</sub> ratio of 5:1, while the hydroxyl radical ·OH was reactive oxygen species on the photocatalytic disinfection using MCNT-TiO<sub>2</sub>.

Additionally, Fu et al. developed onion like carbon (OLC) modified  $\text{TiO}_2$  composite coatings by suspension plasma spraying (SPS) using  $\text{TiO}_2$  and OLC nanoparticles as the starting nanomaterials (Ref 34). Nanostructured features of OLC and  $\text{TiO}_2$  particles were retained in the coatings and unique dispersion of the OLC particles in the coatings was achieved. The authors revealed that the addition of OLC nanoparticles enhanced the photocatalytic performances of the pure  $\text{TiO}_2$ . The synergistic effect of OLC and  $\text{TiO}_2$  particles was further elaborated.

### Metal-Containing Photocatalysts Other than $\text{TiO}_2$

To achieve solar-driven disinfection of waterborne pathogens, a number of efficient, UV to visible-absorptive, metal-containing photocatalysts other than  $\text{TiO}_2$ -based materials have been developed, including ZnO (Ref 35),  $\text{Bi}_2\text{WO}_6$  (Ref 36),  $\text{WO}_3$  (Ref 37),  $\text{Ga}_{0.25}\text{Zn}_{4.67}\text{S}_{5.08}$  (Ref 38), CuI (Ref 39), etc.

ZnO (which has a band gap of 3.37 eV) is abundant in nature, relatively inexpensive and strongly oxidative, which is similar with  $\text{TiO}_2$  when working as photocatalyst. ZnO nanoparticles are widely known for their enormous surface to volume ratio (Ref 40). However, the toxicity of the ZnO nanoparticles in water can pose threats to human health. In order to take advantage of the photocatalytic surface and the safe disposal of ZnO, two ways of immobilization routes are developed. The first is to develop ZnO nanorods on flat substrates (e.g., glass) with seeded ZnO, while the second route is to immobilize the ZnO nanomaterials onto membrane substrates.

As to the first case, Alarcon et al. prepared ZnO nanorods on a glass substrate, from seed layers fabricated from c-irradiated zinc acetate in a thermal bath of a basic zinc nitrate (Ref 41). Sanchez et al. reported immobilized ZnO nanorod films grown on ZnO-seeded polyethylene terephthalate (PET) substrates in alkaline aqueous solution (Ref 42). Rodríguez et al. deposited ZnO-seeded glass substrate by using a spray pyrolysis technique; then, they fabricated ZnO nanorod film from a mixed solution of  $\text{Zn}(\text{NO}_3)_2$  and NaOH. Benefited from larger surfaces of the nanorods, ZnO exhibited good efficiency in bacteria disinfection, and previous measurements showed that the efficiency of ZnO NRs samples correlates with the texture of the nanorod and the number of rods per area (Ref 43).

Ceramic membranes of nano porous anodic aluminum oxide (AAO) were employed to grow highly adherent ZnO nanostructured films (Ref 44). As shown in Fig. 2, Najma et al. developed highly porous networks of ZnO nanosheets on AAO substrate. The membranes were found highly reactive under UV irradiation and greatly deteriorated bacterial population in the nearby vicinity. Moreover, the membranes also showed an appreciable antibacterial

activity in the dark experimental conditions. It was found that the bacterial degradation efficiency of the membranes reached 70% of their efficiency in UV light conditions after 16 h incubation in dark.

Ceramic substrate of clay minerals is another choice for the immobilization of ZnO photocatalyst particles, due to their abundance on earth surface, high porosity, thermal stability, and bio-compatibility. Among different clay materials, kaolinite has been widely used as a cosmetic and healing mineral and is expected to be safe for water treatment application. Ananyo et al. prepared immobilized ZnO nanoparticle photocatalyst on kaolinite substrate, which realized complete disinfection of multidrug resistant *Enterobacter* sp. within 120 min by visible-light-aided photocatalytic disinfection process, exhibiting bactericidal efficiency superior to conventional catalysts such as  $\text{TiO}_2$  and ZnO (Ref 45).

There are some other metal-containing photocatalysts developed in recent years, including  $\text{WO}_3$ , Bi-based photocatalysts (such as  $\text{BiFeO}_4$  and  $\text{Bi}_2\text{WO}_6$ ), several types of binary or ternary sulfides (such as ZnS,  $\text{MoS}_2$ , CdS, and Ga-Zn-S), iodide of precious metals (such as CuI), all of which showed advantages in certain aspects (Ref 46–48).

Nanostructured  $\text{WO}_3$  is a visible-light responsive photocatalyst that absorbs light up to about 480 nm (2.58 eV). It has significant advantages of low cost, harmlessness, and stability in acidic and oxidative conditions. Various strategies, including noble metal deposition, surface hybridization with graphene oxide, were used to promote the photocatalytic activity of  $\text{WO}_3$ . Pt- $\text{WO}_3$  materials realized viral inactivation due to light-induced plasmon (Ref 49). Akhavan et al. incorporated graphene oxide (GO) sheets into  $\text{WO}_3$  films to form graphene- $\text{WO}_3$  (G- $\text{WO}_3$ ) thin films, which was confirmed to be highly efficient in anti-virus use with long-term stability (Ref 50). In the future, it is yet necessary to develop immobilization routes to improve its photocatalytic activity toward practical applications.

Bi-based photocatalysts have been comprehensively investigated recently due to their excellent photocatalytic performance. For example,  $\text{Bi}_2\text{WO}_6$  had a suitable band gap of around 2.8 eV, which was reported as an excellent visible-light-driven photocatalyst for  $\text{O}_2$  evolution or degradation of organic matters. By producing a heterojunction composite by coupling  $\text{Bi}_2\text{WO}_6$  with  $\text{TiO}_2$ , the photocatalytic activity can be greatly enhanced (Ref 51). According to Xu et al.,  $\text{Bi}_2\text{WO}_6/\text{TiO}_2$  composite was successfully prepared by using a one-step hydrothermal method, and demonstrated better photocatalytic bactericidal effect for *E. coli* than single  $\text{Bi}_2\text{WO}_6$  or  $\text{TiO}_2$ . Additionally, Ji et al. synthesized a new ternary composite of  $\text{Bi}_2\text{WO}_6/\text{TiO}_2/\text{rGO}$  by using a facile hydrothermal method for disinfection use (Fig. 3) (Ref 52). The reduced

**Fig. 2** Schematic illustration of photocatalytic degradation of *E. coli* by ZnO/AAO composite membrane (Ref 44)

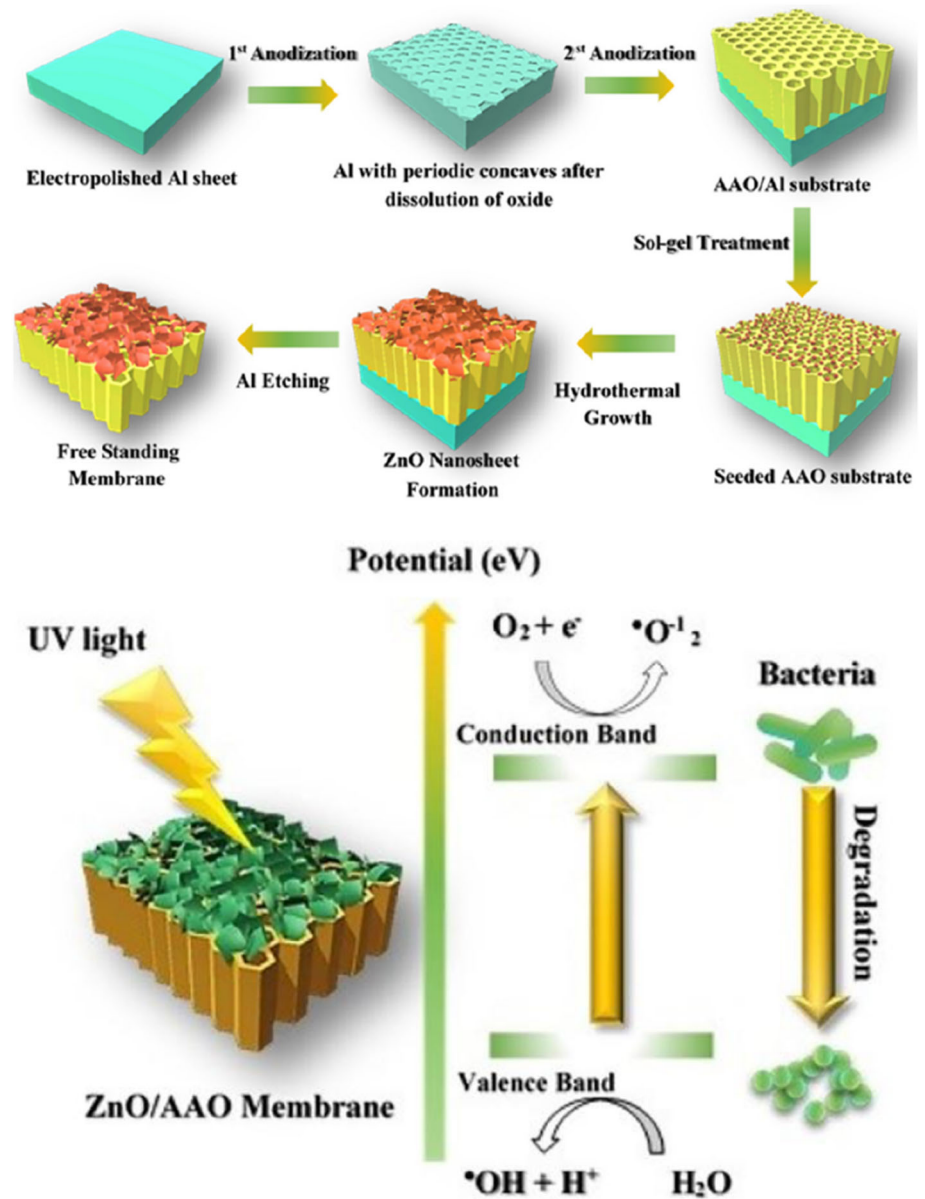
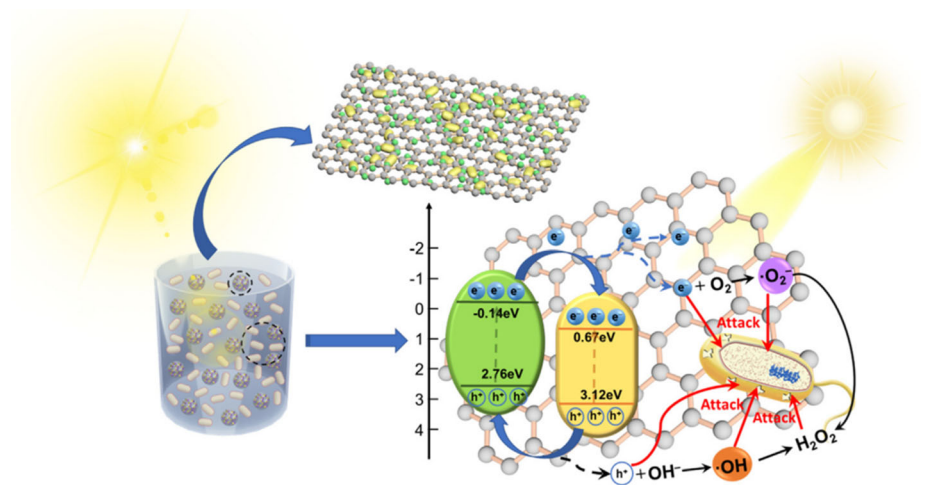


**Fig. 3** Schematic illustration of the underlying photocatalytic mechanism for enhanced disinfection of *E. coli* by Bi<sub>2</sub>WO<sub>6</sub>/TiO<sub>2</sub>/rGO composites (Ref 52)



graphene materials promoted the separation of photocarriers and enhanced the visible absorption, and the  $\text{Bi}_2\text{WO}_6/\text{TiO}_2$  heterojunction gave rise to photogenerated carriers for the disinfection process. The trapping experiments demonstrated that the photoinduced  $\text{h}^+$  played a vital role in the disinfection of *E. coli*, while the derived  $\cdot\text{OH}$ ,  $\text{e}^-$ , and  $\text{O}_2^-$  exhibited synergistic effects. Comparing to  $\text{Bi}_2\text{WO}_6$  or  $\text{TiO}_2$ , the ternary composite material exhibited enhanced visible-light-induced photocatalytic activity against *E. coli*. Moreover, Li et al. reported a Pb-doped  $\text{BiFeO}_3/\text{rGO}$  (reduced graphene oxide) photocatalytic disinfection material which was visible-light-driven and showed high chemical stability. The Pb- $\text{BiFeO}_3/\text{rGO}$  photocatalyst exhibited the strongest bactericidal properties against *E. coli* (100%) and *S. aureus* (99.7%) after 1 h of visible-light irradiation for a 0.5% doping of rGO. High chemical stability was also found even after four reuse cycles (Ref 53).

Binary or Ternary sulfides, such as ZnS, CdS, FeS,  $\text{Ga}_2\text{S}_3$ , and Ga-Zn-S are chemically stable materials, which can be employed for photocatalytic disinfection purpose due to easy synthesis, low cost, high efficiency, and exceptional photoelectric properties. Zinc sulfide (ZnS) has been a research focus recently due to its high negative reduction potentials electrons, excited by UV-visible light. Alafif et al. successfully fabricated zinc sulfide decorated sulfur-doped reduced graphene oxide (S-rGO/ZnS) nanocomposite by using a facile one-pot method (Ref 53). Their results showed that S-rGO/ZnS could effectively absorb visible light which may be ascribed to the heterojunction formation between ZnS and S-rGO, while the S doping in rGO was proven to enhance the electrical conductivity and electron trapping which suppresses the charge recombination. Taking into account the two benefits, S-rGO/ZnS nanocomposite can be utilized under solar light irradiation for the antibacterial process and purification of wastewater.

Cadmium sulfide (CdS) was extensively studied due to its band gap (2.4 eV), corresponding well with the spectrum of sunlight, which makes it active under sunlight or visible light. Furthermore, it is inexpensive and can be easily synthesized through various reproducible methods. Gao et al. reported the fabrication and disinfection performance of graphene oxide (GO)-CdS composites, which were synthesized via a facile two-phase mixing method (Ref 54). The carbon network graphene oxide provides extraordinary conductivity and enlarged surface area, leading to improved photocatalytic disinfection efficiency. Photocatalytic antibacterial activity examination of the GO-CdS composites showed nearly 100% of both gram-negative *E. coli* and gram-positive *Bacillus subtilis* (*B. subtilis*) being killed within 25 min under visible-light irradiation.

The sulfide could also be used as an effective sensitizer for titania photocatalyst because of its high light harvesting efficiency. For instance, Song et al. fabricated titania nanotube arrays which were sensitized with pyrite  $\text{FeS}_2$  by using cathodic electrodeposition of  $\text{Fe}/\text{Fe}_2\text{O}_3$  followed by sulfurizing with evaporative sulfur (Ref 55). The much enhanced visible-light response and photocatalytic performance of the  $\text{FeS}_2$ -sensitized film under the simulated solar light were revealed by the photo-electrical and photodegradation experiments.

Ternary sulfides were found to have narrower band gap and large absorption than  $\text{TiO}_2$  and ZnO catalysts. Among them,  $\text{Ga}_2\text{S}_3$  is an effective optoelectronic material which is stable and easy to adjust by introducing other metals. Yan et al. reported that  $\text{Ga}_{0.25}\text{Zn}_{4.67}\text{S}_{5.08}$  microspheres prepared at 400 °C exhibited the best antibacterial performance, as evidenced by complete killing of *E. coli* K12 within 4 h (Ref 38).

Iodide of precious metals was studied for photocatalytic disinfection use.  $\gamma$  phase CuI possesses smaller band gap (3.1 eV) than  $\text{TiO}_2$  (3.2 eV). Furthermore, CuI adsorbs efficiently heavy metal ions; thus, it can be considered as a good candidate for water treatment. Wojtyla et al. investigated the role of visible-light-induced  $\text{Cu}^+$  to  $\text{Cu}^{2+}$  transition in photocatalytic inactivation of microorganisms (Ref 39). It was found that the photosensitization mechanism encompasses a metal to metal charge transfer. The absorption edge of photosensitized CuI is red shifted toward a lower energy when compared with bare CuI, resulting in enhanced visible-light-induced photocatalytic activity and photoactive in the degradation of organic compounds and inactivation of fungi (*Saccharomyces cerevisiae*).

### Metal-Free Photocatalysts

Although most photocatalysts containing metals or heavy metals have been proven to be excelled in antiviral activity, the accidental leaching of toxic metals, such as Cu and Ag, into treated water could cause serious health concerns. Therefore, there is an urgent need to develop metal-free “green” photocatalyst for inactivation of pathogenic microbes. In the following, we introduce three typical kinds of metal-free photocatalysts developed recently.

As a type of soccer ball-shaped-all-carbon molecule with excelled energy and electron transfer properties,  $\text{C}_{60}$  derivatives can be photoexcited under visible-light irradiation ( $> 2.3$  eV); thus, the material holds promise for photo-reactive applications. When functionalized with hydrophilic moieties, water-soluble  $\text{C}_{60}$  derivatives can be dispersed uniformly in the solution, which can be used as antiviral photocatalysts (Ref 56). The cationic amino  $\text{C}_{60}$  exhibited exceptionally efficient viral inactivation even in

comparison with commercial P25, which is probably due to the electrostatic attraction between positively charged C<sub>60</sub> derivatives and negatively charged MS<sub>2</sub> viruses. The design of C<sub>60</sub>-based photocatalysts for viral inactivation is illustrated in Fig. 4 (Ref 57–60).

Due to the large surface area and good absorptivity in visible band, metal-free GO (graphene oxide) has attracted considerable attention for photocatalysts. By immobilizing aptamers on the edge of GO, Hu et al. synthesized GO-aptamer nanosheets that are highly efficient for anti-virus applications (Ref 61).

Other than photocatalysts based on C<sub>60</sub> and GO, a newly developed graphitic carbon nitride (g-C<sub>3</sub>N<sub>4</sub>) material has been found to be reactive under visible range, biocompatible, resistant to photo-corrosion or air oxidation, and

chemically stable in solvents acids. A major shortcoming of implementing g-C<sub>3</sub>N<sub>4</sub> for practical disinfection use are aggregation phenomena in water and difficulty in separation and recycle. Porous g-C<sub>3</sub>N<sub>4</sub> immobilized on the carrier of natural mineral of expanded perlite (EP) is a new route to tackle these challenges. As shown in Fig. 5, Zhang et al. developed a new composite photocatalyst from low-cost and earth-abundant materials, which possesses several advantages, including highly porous carrier with a large particle size of millimeters, promoting uniform dispersion of g-C<sub>3</sub>N<sub>4</sub> and good reusability, resistant to photo-corrosion, enhanced light utilization, ROS production, and thus antiviral performance. It was reported that the new photocatalyst inactivated all viruses under 240 min visible-

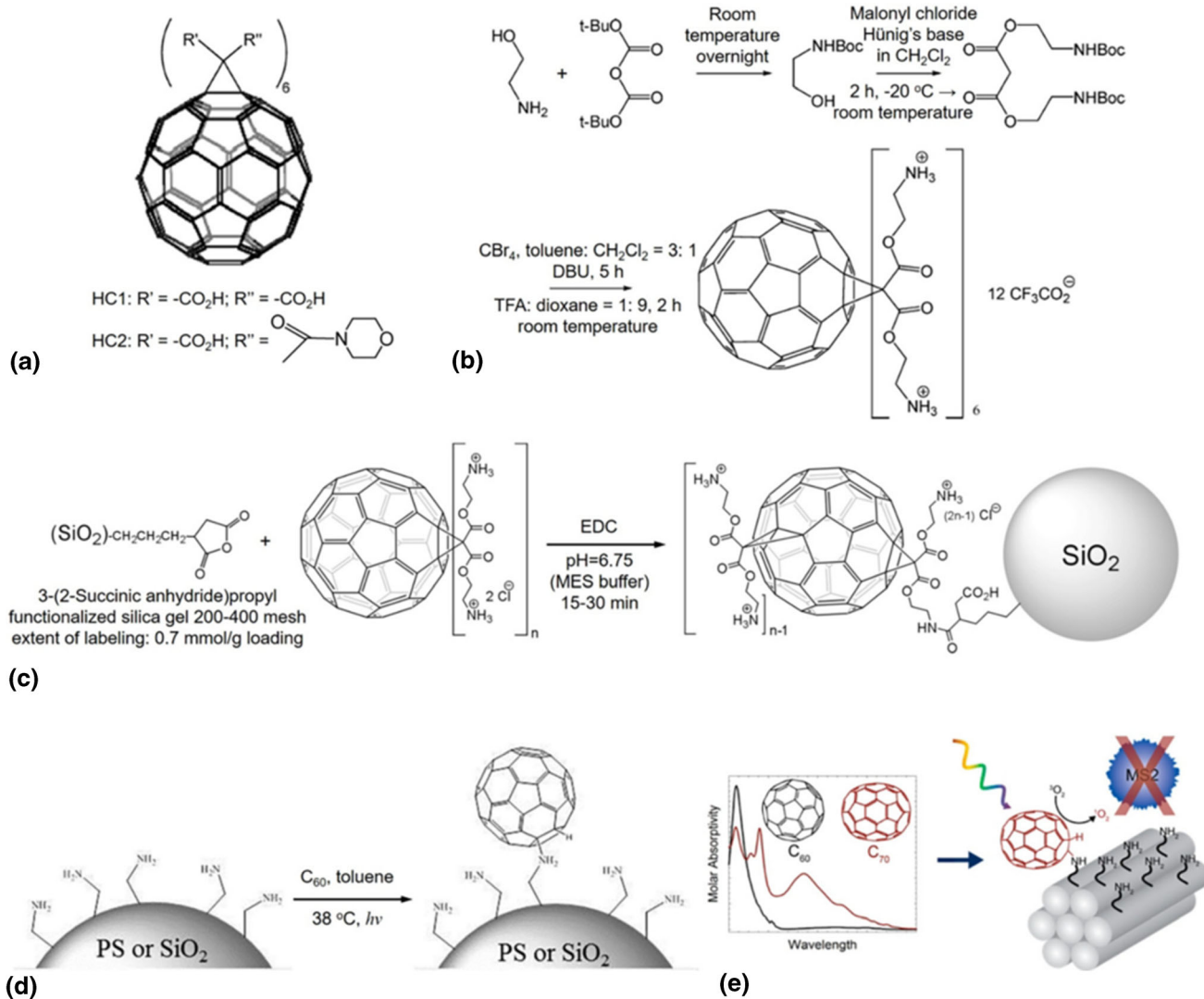
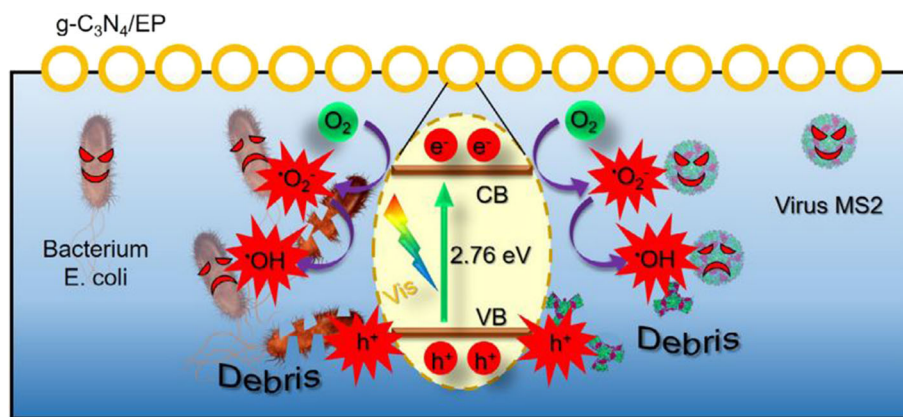


**Fig. 4** Design developments of C<sub>60</sub>-based photocatalysts for viral inactivation: (a) chemical structures of C<sub>60</sub> derivatives (Ref 57), (b) synthesis of cationic amino C<sub>60</sub> (Ref 58), (c) strategy for immobilization of amino C<sub>60</sub> on functionalized SiO<sub>2</sub> (Ref 59),

(d) direct amine addition strategy for immobilization of pristine C<sub>60</sub> on SiO<sub>2</sub> (Ref 56), and (e) UV/Vis spectra of C<sub>60</sub> and C<sub>70</sub> and schematic diagram of viral inactivation induced by C<sub>70</sub>/SiO<sub>2</sub> (Ref 60)

**Fig. 5** Photocatalytic antiviral and antibacterial mechanisms of porous EP/g-C<sub>3</sub>N<sub>4</sub> (Ref 62)



light irradiation (Ref 62), as a comparison, only 77.1% of *E. coli* bacteria can be killed by bulk g-C<sub>3</sub>N<sub>4</sub>.

### Two-Dimensional Photocatalysts

Two-dimensional (2D) nanomaterials have become a rising star in developing photocatalysts for their confined thickness and specific surface area, exhibiting unique structural, physical and chemical properties. Compared to 0D and 1D nanomaterials, 2D nanostructures show obvious superiorities in architecture modulation, charge separation, light harvesting and tunability. There are several merits of 2D photocatalysts. Large lateral size of 2D nanosheets offers plenty of active sites for surface reaction. The plane surface is beneficial for accommodating guest components for the formation of a heterojunction. In addition, the ultrathin thickness promotes the charge diffusion to the surface by shortening the transportation. Moreover, the flexibility of 2D layers enlarges the exposed area for light harvesting. Furthermore, the band gap and absorption of 2D semiconductors are adjustable by simply tuning the thickness of the nanolayers.

Inspired by the unique properties of 2D structured materials, numerous efforts have been devoted to developing highly efficient 2D photocatalysts, as well as exploring their potential in disinfection applications. Many kinds of 2D photocatalysts are being developed recently, including 2D metal oxides, graphene, graphitic carbon nitride, metal oxyhalides, and transition metal dichalcogenides (Ref 63). As typical representatives, the photocatalytic disinfection applications of g-C<sub>3</sub>N<sub>4</sub>, TiO<sub>2</sub>-based photocatalysts and MoS<sub>2</sub> are presented in the following sections.

The photocatalytic efficiency of bulk g-C<sub>3</sub>N<sub>4</sub> is limited by high carrier recombination rate and low surface area. According to Ong, laminar structured g-C<sub>3</sub>N<sub>4</sub> showed several advantages as compared to bulk samples. Further work was carried out by Xu et al., who fabricated porous g-C<sub>3</sub>N<sub>4</sub> nanosheets (PCNS) via a two-step process, i.e.,

hydrothermal treatment and thermal etching (Ref 64). *E. coli* bacteria were completely killed within 4 h by PCNS. In comparison, there are 77.1 and 89.6% of the bacteria still remained during the tests for bulk g-C<sub>3</sub>N<sub>4</sub> and porous g-C<sub>3</sub>N<sub>4</sub> under the same testing conditions. The improved photocatalytic ability was attributed to the improved porosity and enlarged surface area, which facilitate efficient charge carrier separation. Furthermore, the band gap was expanded due to the limited thickness, causing a strengthened photo-redox performance.

Most of the TiO<sub>2</sub>-based photocatalyst for disinfection pertained to the use of nanoparticles, nanotubes or so on. A few studies have been carried out on applying 2D TiO<sub>2</sub>. According to Ma et al., Fe<sub>3</sub>O<sub>4</sub> nanoparticles were deposited on TiO<sub>2</sub> nanosheets (TNS) to serve as an electron acceptor and enable magnetic separation (Ref 65). Bactericidal testing showed a higher microbe removal percentage (92.7% in 2 h) for the hybrid than the pure TNS or Fe<sub>3</sub>O<sub>4</sub>. Increasing the immobility of antibacterial nanomaterials is an important strategy for their reusability. In this regard, Wang et al. coated the TNS onto glass films layer by layer after exfoliating titanium oxide into ultrathin nanosheets, and then, the device was used for photocatalytic microbe inactivation (Ref 66). The extraordinary thin coating layer was nearly transparent in UV–Vis spectrum. However, the functional photocatalytic layer could still perform disinfection effect when illuminated, which was attributed to the electron storage ability of the multi state Ti. The photocatalytic film was effective after 5 cycles of operation, indicating its good potential for water purification. Moreover, Zhang et al. reported a TiO<sub>2</sub>-based catalytic film with dark inactivation ability. A layer of TiO<sub>2</sub> seeds was firstly deposited on glass using sol–gel method. Then, the TiO<sub>2</sub> seeds grew onto Ag-embedded parallel nanosheets after solvothermal treatment in TiO<sub>2</sub> and AgNO<sub>3</sub> sol, forming a catalytic coating on the glass surface (Ref 67). The photocatalytic film exhibited bactericidal performance of almost 100% (365 nm, 24 h), and it also achieved a sterilizing rate of above 99% to both gram-negative and gram-

positive bacteria in dark. The Ag particles played a dual role in the antibacterial process: electron acceptor and cytotoxicity.

Few-layered MoS<sub>2</sub> nanosheets (NSs) have the advantages of being able to harvest the whole spectrum of visible light (approximately 50% of solar energy) and have been reported to effectively generate photocatalytic reactions, which presented superior catalytic activity and disinfection performance owing mainly to prolonged electron-hole pair (EHP) lifetime. Chou et al. (Ref 68) reported a single- and few-layered MoS<sub>2</sub> decorated with Au nanoparticles (NPs) as a new efficient nanocatalyst that can be simply activated by ambient mechanical force and light excited electron-hole pairs, as shown in Fig. 6(a). After deposition of Au NPs, ~ 99.999% reduction in bacteria can be achieved by visible-light irradiation for 60 min, while the required treatment time can be reduced to 15 min under a combination of mechanical vibration and IR light irradiation (Fig. 6b, c, and d).

### Thermal-Sprayed Photocatalytic Coatings

The photocatalytic particles can be used for disinfection of a wide range of microbes (e.g., pathogenic bacteria, viruses, and fungi) with the advantages of ease in use and high efficiency. However, the suspended photocatalytic powers have the shortcomings including difficulty in separation and recycling. Moreover, leakage of the photocatalytic nanomaterials in most cases may cause secondary pollution. Therefore, practically, the photocatalytic nanoparticles should be immobilized onto the surface of a certain substrate (e.g., quartz, steel, polymer, etc.) in a large scale so as to produce mechanically stable coatings. Thermal spray photocatalytic techniques offer the advantages of low

cost, wide selection of coating materials, and easy on-site operation, making it promising for the fabrication of large-scale photocatalytic coatings. Divided by different working modes, the thermal spray techniques include but are not limited to atmosphere plasma spray (APS), suspension plasma spray (SPS), flame spray, high-velocity oxy-fuel (HVOF) spray and cold spray, which are important in photocatalytic disinfection applications (Ref 69-71). A novel low pressure cold gas spraying technique was used to large-scaled fabrication of carbon-modified TiO<sub>2</sub> photocatalytic coatings as shown in Fig. 7. In this section, the fabrication methods, coating microstructures, as well as the photocatalytic disinfection mechanisms, performances and applications of thermal-sprayed coatings in eight different emerging trends are reviewed.

### Visible-Light-Induced Photocatalytic Coatings

There is only ~ 4-5% of solar light being within the UV range, while the visible light contributes about 50% of the total power. Therefore, many attempts were made to attain visible-light-induced photocatalytic activities, for instance, structure modification, metal and nonmetal doping, co-deposition of metals, and mixing of two semiconductors (Ref 72-75).

The visible absorbance of the photocatalysts can be greatly improved by using modified TiO<sub>2</sub> powders or nanotubes via different synthesis routes, leading to improvement in disinfection efficiency. According to Birben et al., N-doped, Se-doped, and Se-N co-doped TiO<sub>2</sub> showed visible light activated photocatalytic disinfection efficiency (Ref 76), whereas undoped TiO<sub>2</sub> displayed comparatively slower removal rates of *E. coli* than the doped and co-doped TiO<sub>2</sub> specimens. Additionally, Koklic et al. investigated the visible driven photocatalytic

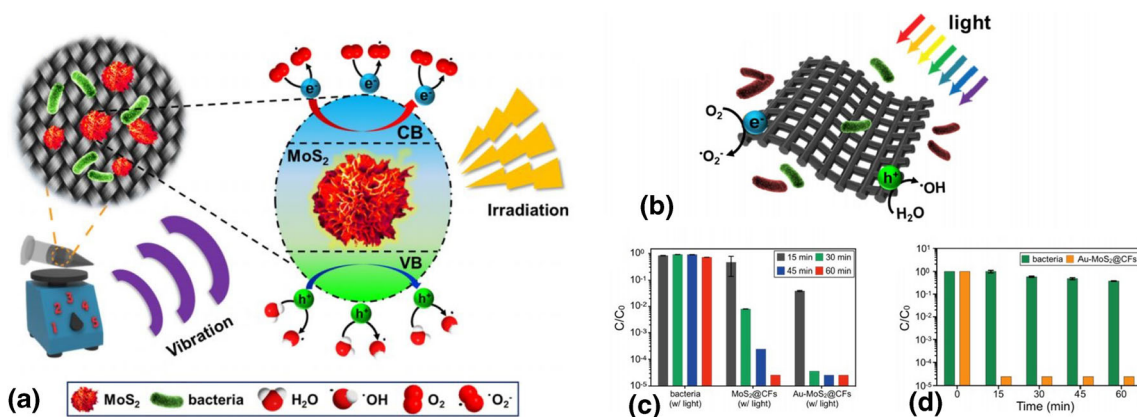


**Fig. 6** (a) Schematic diagram of the Au-MoS<sub>2</sub> nanocatalyst for water disinfection application. (b) Illustration of Au-MoS<sub>2</sub>@CFs achieving bacterial disinfection under light irradiation. (c) Disinfection performance of the control (pure bacteria), MoS<sub>2</sub>@CFs and Au-MoS<sub>2</sub>@CFs

under visible-light irradiation. (d) Disinfection performance of Au-MoS<sub>2</sub>@CFs under a combination of mechanical vibration and IR light irradiation (Ref 68)

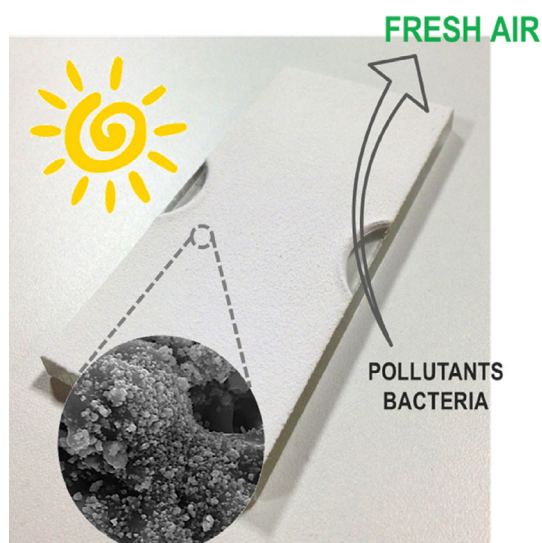


**Fig. 7** Top surface of the cold-sprayed carbon-modified TiO<sub>2</sub> photocatalytic coating (Ref 71)

disinfection properties of copper-doped TiO<sub>2</sub> nanotubes deposited on existing surfaces. It was found that the ceiling mounted fluorescent light can retard the growth of *Listeria innocua* by 80% in 7 h of exposure to fluorescent light (Ref 77). Furthermore, Feilizadeh et al. prepared Fe-Cd co-doped photocatalytic powders to realize the inactivation process by visible light. Based on the experimental data and a semi-empirical model, the authors predicted that the Fe-Cd/TiO<sub>2</sub> catalyst was able to achieve a bacterial inactivation efficiency of 99.9% after 45 min of visible-light illumination (Ref 78).

For practical disinfection application, researchers have used thermal-sprayed TiO<sub>2</sub> coatings. According to Bettini, an anatase/rutile mixed-phase photocatalyst was reported in the form of nanostructured powders by flame spray pyrolysis (FSP) method (Ref 79), which showed photocatalytic activity under sole visible light, indicating the potential of the FSP-made powders as indoor photocatalysts for disinfection purposes. A more practical study by M. Nararom et al. was conducted using a thermal-sprayed TiO<sub>2</sub> coating on plates (Ref 80). A parabolic concentrator to enhance the power density of the solar radiation for the disinfection of water containing *E. coli*. Acrylic matt black spray was used to prepare black reactor, which was proved to be more efficient for the inactivation of bacteria due to higher efficiency in absorbing photons to damage the bacteria. By using an optimized setup, effective inactivation of bacteria by approximately 4 logs were achieved within 90 min.

Doping with metals or constructing heterostructures were considered to be beneficial to the visible-light-induced photocatalytic activity or disinfection efficiencies. According to P. Ctibor et al., iron-doped TiO<sub>2</sub> coatings

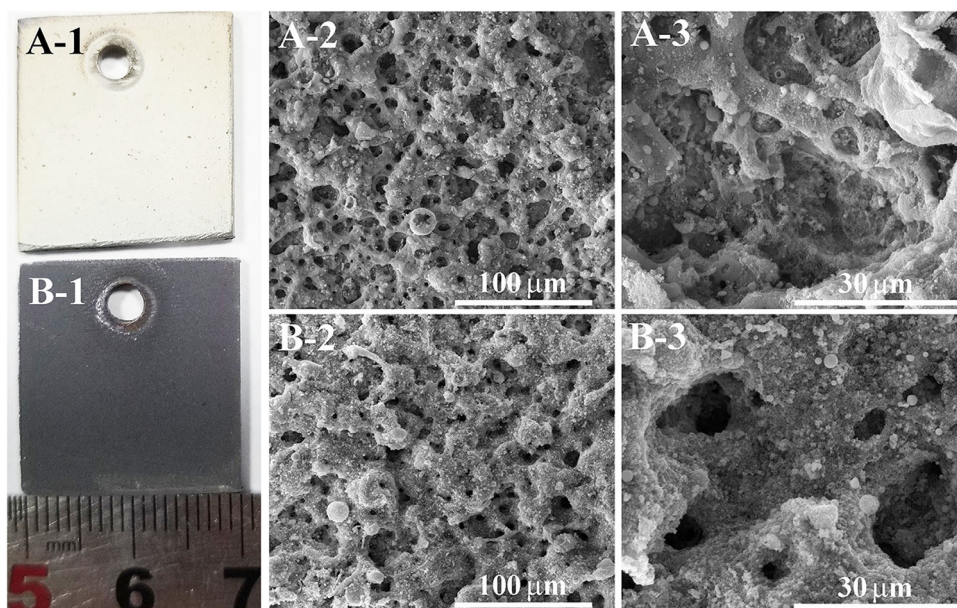
were prepared using atmospheric plasma spraying method with water- and gas-stabilized guns (Ref 81). Presence of FeTiO<sub>3</sub> was detected in water-stabilized plasma sprayed coatings, which were more photocatalytically active than undoped coatings. In comparison, hydrogen-rich atmosphere in the gas stabilized plasma spray led to the reduction of certain amount of iron oxides to metallic iron. Consequently, the charge-transfer transition by UV or visible excitation between dopant ions via the conduction band took place in the coating, leading to improvement in butane conversion. However, the disinfection performance of the coatings was still unreported. George et al. reported that flame sprayed Cu-doped TiO<sub>2</sub> coating contained limited anatase phase due to the high growth temperature, while it still killed approximately 75% of PAK bacterial cells after 3 h under white light illumination (400–700 nm), showing the same bactericidal capabilities as pure copper surfaces. Hence, the toxicity of Cu could exhibit synergistic effect with photocatalysis in disinfection applications (Ref 82). Moreover, Zhai et al. reported suspension plasma sprayed TiO<sub>2</sub>-SrCO<sub>3</sub> heterostructure nanomaterial coatings for visible-light-induced disinfection, which exhibited superior bactericidal activities against *E. coli* to that of the pure TiO<sub>2</sub> coatings, achieving a killing rate of over 99.7% within about 4 h (Ref 83).

### Black TiO<sub>2</sub> Photocatalytic Coatings

TiO<sub>2</sub> is one of the most widely used photocatalysts; however, the wide band gap of TiO<sub>2</sub> (3.2 and 3 eV for anatase and rutile TiO<sub>2</sub>, respectively) and rapid charge recombination are the main shortcomings toward its practical applications. Extensive efforts were made to achieve visible-light photocatalytic activity through constructing intrinsic defects or making doping. Among the modified TiO<sub>2</sub>, black TiO<sub>2</sub> showed excelled absorptivity in ultra violet to infrared range and were widely used for solar energy utilization (Ref 84), photodegradation (Ref 85), electrocatalysis (Ref 86, 87), among others.

It was recently realized that black TiO<sub>2</sub> has much better photocatalytic activities than other structured TiO<sub>2</sub>. Zhou et al. synthesized a series of nitrogen-doped black TiO<sub>2</sub> nanocatalysts via a one-step method. It was found that the urea addition inhibits the anatase to rutile phase transformation and also the formation of black TiO<sub>2</sub> by N doping. The black TiO<sub>2</sub> had more efficient excited charge separation and higher photocatalytic efficiency for *algae* inactivation (Ref 88). Furthermore, to facilitate the application of black TiO<sub>2</sub>, Zhai et al. fabricated black TiO<sub>2</sub> coatings by using a suspension plasma spray (SPS) method. Black TiO<sub>2</sub> coatings with porous microstructures and high photocatalytic activity were realized (Ref 21), as shown in Fig. 8. The high temperature during the spray processing triggered

**Fig. 8** Digital photographs and topographical morphology of the white TiO<sub>2</sub> coating (A) and the black TiO<sub>2</sub> coating (B) fabricated by suspension plasma spraying. (-3 is enlarged view of selected area in -2) (Ref 21)



partial structure transformations of anatase to rutile, brookite, and remarkable lattice disorders of anatase, which significantly narrowed the band gap to 2.71 eV. The enhancement in solar absorption therefore increases its photocatalytic efficiency.

### Porous Heterostructured Photocatalytic Coatings

Porosity is a vital factor that influences photocatalytic performances of photocatalytic coatings. Photocatalytic disinfection efficiency of porous photocatalyst is usually desired, for large surface area usually facilitates multiple light scattering effect and accelerated diffusion of ion species. Porous structures also lead to improved efficiency in generating ROSs products (e.g., O<sup>2-</sup>, H<sub>2</sub>O<sub>2</sub>, holes) that are crucial for bacteria inactivation. For viral and fungal inactivation, porous surface can shorten the diffusion pathway of the short-lived radicals (e.g., ·OH) with high oxidizing power and promote their concentration, which are vital for the denaturing process of the rigid protein shells of virus, or the cell wall of fungi. Moreover, porous photocatalyst offers plenty of sites for anchoring active nanoparticles (NPs). Formation of the photocatalyst-NPs heterostructures will improve the separation efficiency of charge carriers and production of ROSs, which largely enhances the photocatalytic disinfection efficiency.

There is a number of routes to increase the porosity of the photocatalysts, including choosing organic fibers or mesoporous substrates, or synthesize microsphere shaped particles. According to Xu et al., TiO<sub>2</sub> nanowires were precipitated on polyester fabrics through multi-steps of surface roughening, sol-gel TiO<sub>2</sub> seeding, hydrogen titanate nanobelts precipitation, and sulfuric acid treatment

(Ref 89). Both mesoporous anatase TiO<sub>2</sub> nanowires and single-crystalline rutile TiO<sub>2</sub> nanorods have been achieved, which exhibited remarkable sterilization of *E. coli* and *S. epidermidis*. Additionally, Purbia et al. synthesized C-doped anatase TiO<sub>2</sub> multi-tubes by using banana stem fiber as sacrificial template. High surface area ( $\sim 99 \text{ m}^2/\text{g}$ ) with a mesoporous structure made of  $\sim 15 \pm 3 \text{ nm}$  nanoparticles were reported, which exhibited enhanced light absorption property in visible region and excellent photocatalytic activity (Ref 90). Furthermore, Zhang et al. prepared porous g-C<sub>3</sub>N<sub>4</sub> by loading graphitic g-C<sub>3</sub>N<sub>4</sub> onto expanded perlite (EP) support through a facile hydrothermal process. EP/g-C<sub>3</sub>N<sub>4</sub> exhibited excellent antibacterial activity against *E. coli* (8-log reduction) and antiviral activity (*MS2 phage*) under visible-light exposure of 180 and 240 min, respectively (Ref 62). Yan et al. reported that Ga<sub>0.25</sub>Zn<sub>4.67</sub>S<sub>5.08</sub> microspheres prepared at 400 °C exhibited the best antibacterial performance, which attained complete killing of *E. coli* K12 within 4 h. The authors attributed the superior photocatalytic activity to high specific surface areas and narrowed band gap (Ref 38). All these studies improved the disinfection performance of the photocatalyst by taking advantage of the high porosity.

Developing micro/mesoporous surface and visible active photocatalysts on a large scale is a promising task from the practical perspective. Thermal spray is an important fabrication route to realize porous photocatalytic structures. Recently, some researchers focused on the doping/processing-porosity-property correlation of thermal-sprayed TiO<sub>2</sub> coatings. It was found that their photoactivity was comparable favorably to that of chemical vapor deposition (CVD) coatings and compressed P25 disks, where the bimodal-sized porosity was believed to be

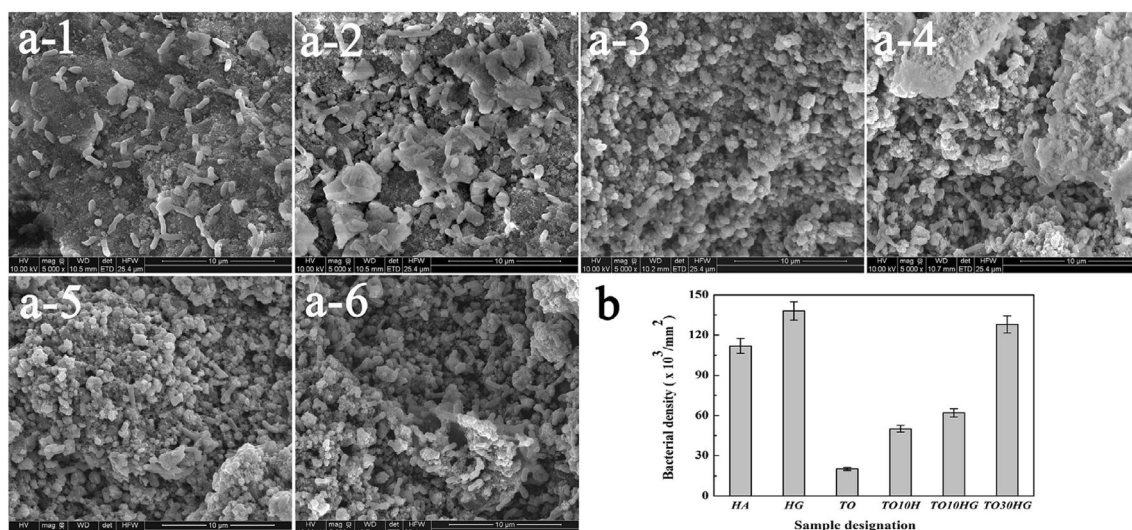


**Fig. 9** Addition of HA-rGO in TiO<sub>2</sub> coatings effectively increases the specific surface area of the coatings and markedly enhances recruitment of *E. coli* for subsequent photocatalytic elimination. (a) SEM images of *E. coli* adhered on the coatings after incubation for 6 h; -1: the pure HA coating, -2: the HA-rGO coating, -3: the pure

titania coating, -4: the TiO<sub>2</sub>-10 wt.% HA coating, -5: the TiO<sub>2</sub>-10 wt.% (HA-rGO) coating, -6: the TiO<sub>2</sub>-30 wt.% (HA-rGO) coating, and (b) bacterial density as determined by statistical counting of the *E. coli* adhered on the surfaces of the coatings (Ref 100)

optimal for desired photocatalytic performances (Ref 91, 92). Sugiyama et al. fabricated porous TiO<sub>2</sub> coatings with uniform porosity along depth direction by a modified spray pyrolysis deposition (SPD) technique, where the porous surface with an effective area eight times higher than that of the non-porous sample was achieved. Consequently, the photocatalytic ability was enhanced by 2.5–2.8 times (Ref 93). Additionally, Jbeli et al. investigated the synthesis and physical properties of Fe-doped La<sub>2</sub>O<sub>3</sub> coatings grown by spray pyrolysis with a doping rate of 0–5%. The optimal photocatalytic activity was reached at the doping rate of 4%, due to its dispersed and distorted porous structure constituted by small nanoparticles (Ref 94). Moreover, Zhang et al. found that the lower plasma power and higher powder feeding rate resulted in formation of higher porosity content in the plasma sprayed TiO<sub>2</sub> coating, where the porosity has a dominating effect deciding the photocatalytic performance (Ref 95). The improvement in the photocatalytic performance of these porous coatings were proved via photodegradation of the subject matters, where the photocatalytic disinfection ability of the coatings is yet to be reported.

Therefore, for versatile environmental applications, extensive research efforts have been devoted to achieving large-scale photocatalytic coatings. According to Lin et al., mesoporous TiO<sub>2</sub> nanocrystalline (NC) membranes with average pore size of 0.35 μm were successfully fabricated by coating on an alumina support via a rapid atmospheric plasma spray (APS) approach (Ref 96). The photodegradation experiments of dextran and humic acid prove its potential in photodegradation of bio-organisms and protein

under UV light irradiation, which is essential in photocatalytic disinfection. Additionally, M. C. Bordes prepared TiO<sub>2</sub> photocatalytic coatings by APS from different feedstocks (Ref 97). The feedstocks were obtained by spray drying suspensions of a nano- and a submicron-sized TiO<sub>2</sub> powder, with different solids contents and/or ratios of the nano- to submicron-sized particles. It was revealed that the coating porosity as well as the amount of partially melted areas depended strongly on plasma spray conditions and on feedstock characteristics. In another work, Kim et al. investigated the photocatalytic property of plasma sprayed TiO<sub>2</sub> coating on foamed waste-glass substrates (Ref 98). The porous coating sample was found to be efficient in purify the green tide and the red tide when illuminated by UV light, where the nano-sized commercial TiO<sub>2</sub> particle and mesoporous structure of the foamed glass improve the photocatalytic efficiency. Moreover, Mcfarlane et al. studied the sterilization mechanism of three different microbes (*P. aeruginosa*, *S. aureus*, *C. albicans*) by using jet spray formed titanium dioxide surfaces (Ref 99). The authors point out two important factors that are responsible for the high efficiency of inactivation: the high surface area of the porous nanomaterial and the direct contact between the microorganisms and the UV-activated surface. Furthermore, Zhai et al. reported suspension plasma sprayed TiO<sub>2</sub>-SrCO<sub>3</sub> heterostructure nanomaterial coatings for the first time (Ref 83). The TiO<sub>2</sub>-SrCO<sub>3</sub> co-catalyst with semiconductor heterostructures show significantly superior bactericidal activities against *E. coli*, which is partly attributed to the novel porous structure of the coating.

## Bacteria Recruitment and Killing Strategies

To achieve effective sterilization, the photocatalytic material must essentially favor the attachment of bacteria because of the short lifetime and diffusion length of the released ROSs. Support for the photocatalytic nanoparticles is able to limit the aggregation phenomena of the particles and contribute to the efficient spatial separation between the photogenerated electrons and holes. Therefore, by using the biocompatible supporting materials (e.g., zeolite, perlite, hydroxyapatite (HA), reduced graphene oxide (rGO), etc.) as baits, the recruitment and killing strategies have been a research focus. The bactericidal effect can be improved by enhancing the adsorption of bacteria and optimizing the ROSs radical generation on the supports by using these strategies (Ref 100–105).

Zeolites are crystalline aluminosilicates with regular dimension structure, channels and cavities called micropores, which can be used as the bait of the recruitment. Reddy et al. investigated the photocatalytic bactericidal activity of TiO<sub>2</sub> supported over different support systems of HY, H $\beta$ , HZSM-5 and SiO<sub>2</sub>-Al<sub>2</sub>O<sub>3</sub> systems (Ref 101). It was observed that H $\beta$  zeolite exhibited the most mechanical adsorption of negative surface charged bacterial cells among the selected supports, which in turn enhanced the bactericidal activity given by ·OH radicals generated by photocatalytic TiO<sub>2</sub> under light irradiation. Based on the experimental results, 5 wt.% TiO<sub>2</sub> loading over H $\beta$  is sufficient to get higher bactericidal activity in comparison with TiO<sub>2</sub> solely. The shortcoming is that the samples were prepared by mixing the supports with TiO<sub>2</sub> in an agate mortar using dry ethanol, which limits its yields for practical application.

Thermal spray method has been used to prepare composite materials of support and photocatalysts in a large scale. As a highly porous and chemically inert media, perlite granules can act as a good adsorbent and support for TiO<sub>2</sub> photocatalysts. M. Giannouri et al. presents the one-step synthesis of the TiO<sub>2</sub>/perlite composites by flame spray pyrolysis (FSP) processing. The composite samples exhibited improved photocatalytic activity in comparison with commercial TiO<sub>2</sub> P25. However, the disinfection performance of TiO<sub>2</sub>/perlite composites is yet to be reported (Ref 102) TiO<sub>2</sub>-hydroxyapatite (HAp) hybrid films were proved to be candidates for photocatalytic decomposition of germs, viruses by Nakajima et al. through spray pyrolysis deposition (SPD) method (Ref 103). Liu et al. prepared photocatalytic TiO<sub>2</sub>-HA coatings with significantly promoted adherence of *E. coli* bacteria (Ref 104), since HA is essentially biomedical material that bacteria like to stay on. It was also revealed that the coatings consisting of 10 wt.% HA showed the best photocatalytic activity, which is comparable to that exhibited

by immobilized Degussa P25 coating. However, the photocatalytic disinfection mechanisms of *E. coli* were not discussed in the study. To further investigate the antibacterial mechanism, Huang et al. fabricated two types of TiO<sub>2</sub>-HA nanocomposites (TiO<sub>2</sub>-HA, TiO<sub>2</sub>-HA-rGO) by liquid flame spray deposition (Ref 100, 105). HA-enwrapped TiO<sub>2</sub> nanocomposite powder was fabricated by using P25 particles as nucleation sites. HA in the composite powder acts as bait attracting approaching of bacteria and pushing them to TiO<sub>2</sub>. Moreover, the vacancies formed on the surface of excited phosphate group (PO<sub>4</sub><sup>3-</sup>) in UV illumination might lead to formation of superoxide radical (O<sup>2-</sup>), which also attacks the surrounding bacteria adsorbed on HA. As a result, the HA layer promoted significantly recruitment of *E. coli* bacteria onto the TiO<sub>2</sub>-based particles for subsequent photocatalytic killing, which gave rise to better capability of photocatalytic sterilization (Fig. 9).

## Thermal Spray Fabrication of Hollow Structured Photocatalysts

The morphology of TiO<sub>2</sub> particles influences their performance of photocatalytic viral disinfection. It is known that suspended reactors are more efficient than immobilized ones due to large surface area available for redox reactions. For instance, TiO<sub>2</sub> hollow particles showed promoted photocatalytic performance than spherical ones in degradation of *dimethyl sulfoxide* due to the multi-scattering of light inside the hollow structure that could increase light absorption (Ref 106). However, the main drawback of using nano- or micro-sized particles in suspension is the necessity of post separation treatment or recycling of the catalyst, potentially making the use of the catalyst more complex and expensive.

To overcome the shortcoming of reusability of suspended reactors, researchers fabricated hollow microspheres of TiO<sub>2</sub> that were easy to reuse. Ren et al. reported a suspension plasma sprayed hollow microsphere of TiO<sub>2</sub>-Fe<sub>3</sub>O<sub>4</sub> composites, exhibiting excellent photocatalytic performance and good reusability. Due to the presence of magnetic Fe<sub>3</sub>O<sub>4</sub> nanoparticles in the TiO<sub>2</sub> hollow spheres, the micro spheres can be easily recycled through external magnetic field (Fig. 10). Excellent photocatalytic sterilization performances were revealed for the TiO<sub>2</sub>-Fe<sub>3</sub>O<sub>4</sub> hollow microspheres (Ref 107, 108). After 5 h UV irradiation, ~ 99% bacteria were already exterminated. The addition of Fe<sub>3</sub>O<sub>4</sub> did not deteriorate the photocatalytic performances of the TiO<sub>2</sub> hollow spheres. Additionally, a special design of FeO<sub>x</sub>-TiO<sub>2</sub> nano composites was proposed (Ref 109), which resolved the problem of reusability of the photocatalytic particles. According to the study of

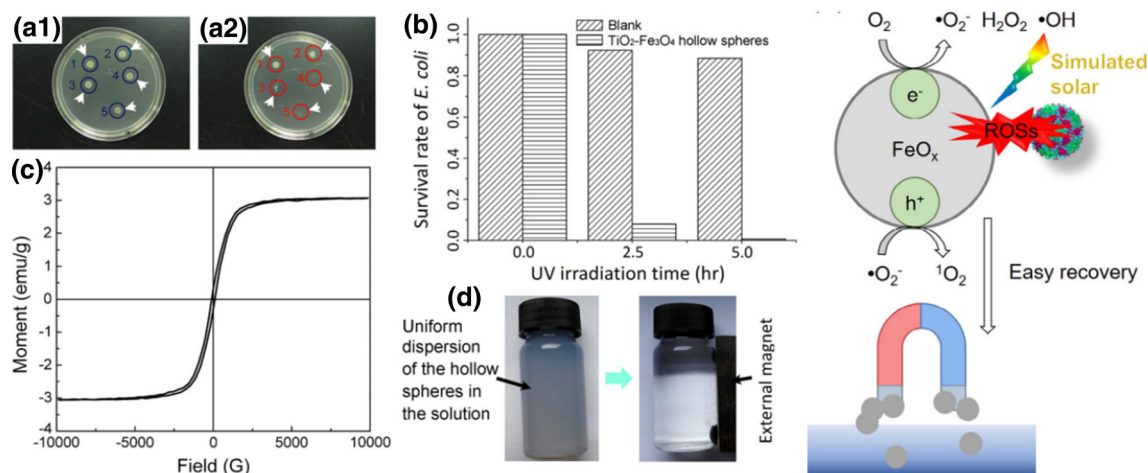


**Fig. 10** Recyclable iron oxides-containing photocatalysts for bacterial (left) (Ref 107) and viral inactivation (right) (Ref 109)

Giannakis et al., three types of iron oxides (wüstite, maghemite, nano-maghemite) showed photocatalytic antiviral activity under solar irradiation (Fig. 10) (Ref 109). Particularly for wüstite, it exhibited the highest inactivation efficiency in both ultrapure water and wastewater, achieving 5-log MS<sub>2</sub> inactivation in 30 min and 2.6-log MS<sub>2</sub> inactivation in 120 min, respectively.

### Superhydrophobic Self-Cleaning Photocatalytic Coatings

Self-cleaning surfaces have attracted attention due to their potential use in anti-bacteria and antifouling purposes (Ref 110, 111). Photocatalyst coating with self-cleaning property combines dual functions of antibacterial effects: anti-adhesive/self-cleaning surfaces and photocatalytic sterilization, which prevents the adherence of antibiotic-resistant bacteria and the formation of biofilms. Many researchers have reported various photocatalyst coatings constructed by using superhydrophobic or low energy surfaces, which can be used in a variety of fields including the reduction of HAIS (healthcare associated infections), marine antifouling, food industry, etc.

Self-cleaning photocatalyst coatings were fabricated by a number of techniques. According to He et al., a series of ZnO-rGO nanocomposite films were prepared by sol-gel technique. The ZnO-rGO films possess photocatalytic activity and photoinduced superhydrophilicity, and increased content of rGO enhanced both photocatalytic activity and photoinduced superhydrophilicity of the ZnO-based films (Ref 112). For reduction of HAIS, Won et al. prepared TiO<sub>2</sub>-based transparent coatings as one such potential self-cleaning surface for touch screen application and evaluated their antimicrobial efficacy under dark and illuminated conditions (Ref 113). It was revealed that n-Ag/TiO<sub>2</sub> (< 100 nm) coated samples achieved greater

than 80% bactericidal efficacy with the lowest bacterial attachment after UV exposure (Ref 113).

To explore the industrial potential of the self-cleaning photocatalyst, researchers have recently attempted to develop hydrophobic/superhydrophobic surfaces by thermal spray processing. For instance, Teisala et al. developed a nanostructured TiO<sub>2</sub> coating deposited on top of paper-board using liquid flame spray with a roll-to-roll setup at ambient pressure, which has potentials in using as self-cleaning surfaces (Ref 114). Valenzuela et al. prepared photoactive coatings using sol-gel ZnO suspensions through electro-spraying on glass substrates, and self-cleaning antimicrobial functions were reported (Ref 115). The electro-sprayed surfaces displayed antibacterial activity against *Staphylococcus aureus* with a reduction rate of over 99.5%.

Because of the difficulty in constructing desired topographical nanostructures, insufficient hydrophobicity hinders the application of thermal spray in fabricating superhydrophobic coatings. An innovative method was proposed by Huang, et al. for plasma spray deposition of superhydrophobic coating by using Al@WO<sub>3</sub> core-shell powder as the feedstock (Ref 116). Two nano-products (Al<sub>2</sub>O<sub>3</sub> and W) were formed on the top layer of the coatings, as a result of transformation of WO<sub>3</sub> to W during the spraying processing. They claimed that the acidic conditions facilitated the photocatalytic activity of the coatings. Co-existence of super hydrophobicity and photocatalytic performance suggests the potential antibacterial and antifouling applications of the thermal-sprayed coatings (Ref 116).

### Anti-biofilm Photocatalytic Coating

Biofilm-related infections are predominately responsible for the spreading of many infectious diseases, particularly

in the case of medical devices, foodborne diseases, and cause huge economic loss. Increased resistance to conventional antibiotics of pathogenic microbes requires the importance of developing alternative strategies for preventing pathogen dissemination. To construct anti-biofilm photocatalytic coatings, apart from the coating technique, understanding the mechanisms as to how surface characteristics of photocatalytic coatings influence the formation of the biofilms is essential.

A study by Jalvoa et al. on the influence of typical surface characteristics of TiO<sub>2</sub>-functionalized material on the formation of biofilms revealed that the biofilm-forming bacteria *Staphylococcus aureus* and *Pseudomonas putida* grew easily on TiO<sub>2</sub>-functionalized filters (Ref 117). The ROS products generated by the irradiation of visible-near UV light can kill all cells, while they were unable to remove the biofilm matrix formed during prior dark period. In a comparison study on bacterial cells death on 304 steel and TiO<sub>2</sub> coatings conducted by McDonald et al. (Ref 118), it was revealed that 24% of the *Pseudomonas aeruginosa* bacterial cells on HVOF sprayed TiO<sub>2</sub> coatings were killed after exposure to white light, comparing to merely about 6% on stainless steel surface. In contrast, Kikuchi et al. found that TiO<sub>2</sub> thin films can kill 100% of *E. coli* bacteria after exposure to UV radiation (Ref 119). Therefore, McDonald et al. claimed that the difference is probably due to the ability of the *Pseudomonas aeruginosa* bacteria to form and embed themselves in biofilm matrix (Ref 118).

### Different Surface Topographies of ZnO Photocatalytic Coatings

Topography of ZnO coatings influences their photocatalytic activities (Ref 120). To construct superior structure for modified electron band, Chen et al. made nano-ZnO coatings with porous topographical morphology through liquid plasma spraying. The coatings showed a porous skeleton and a fluffy top layer consisting of ultrafine ZnO grains, exhibiting a narrowed band gap and modified oxygen defects as compared to those deposited from single liquid feedstock (Ref 121). As reported by Heinonen, ZnO films with three topographies: needle-like hexagonal rods and flakes showed distinctive photocatalytic efficiency, which is proportional to their active surface area (Ref 122). Additionally, Rodríguez et al. used the spray pyrolysis (SP) technique to prepare different seed layers which plays a vital role in regulating crystalline growth and order of ZnO nanorods for the photocatalytic coatings (Ref 123). Higher surface area nanorods were preferentially synthesized in the samples prepared from the seed layer at pH 4, which was considered to be the main parameter influencing the bacterial inactivation.

Finally, a comparison on the photocatalytic disinfection efficiency of thermal-sprayed photocatalytic coatings is summarized in Table 1.

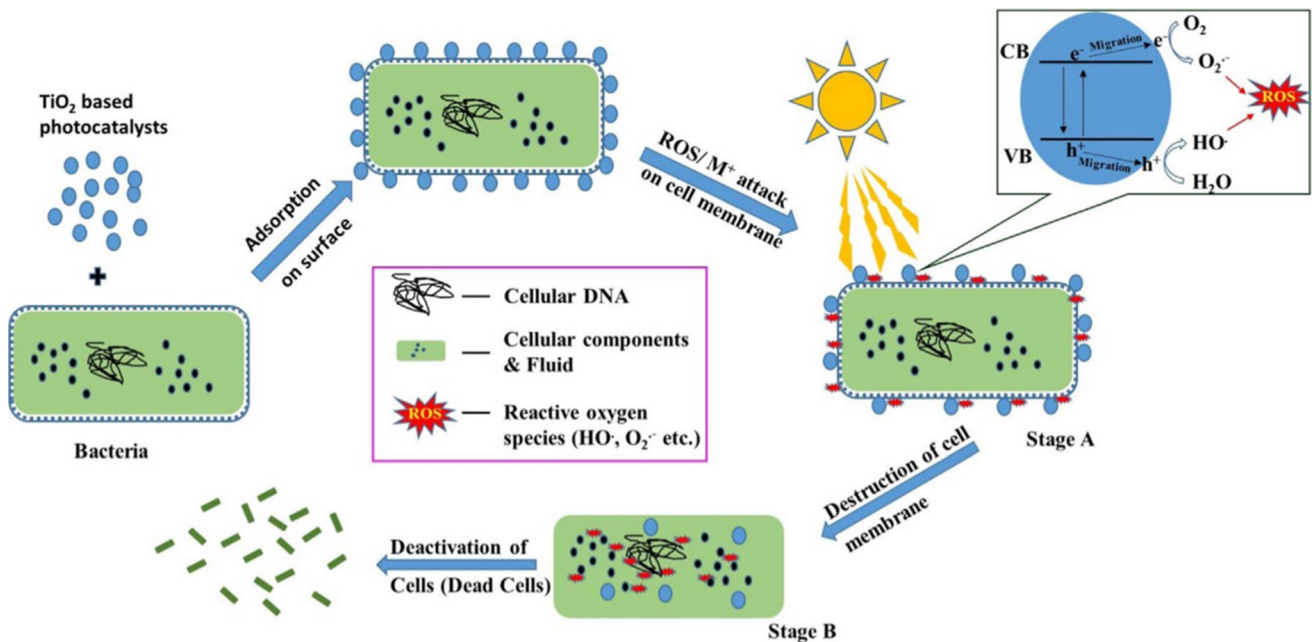
### Photocatalytic Disinfection Mechanisms

A variety of factors may influence the photocatalytic disinfection efficiency, including temperature, pH value of the aqueous solution, dissolved oxygen, light intensity, etc. Apart from the objective conditions, the inner mechanisms of photocatalysis are more important for the disinfection properties, including the roles of the photocatalysts in the disinfection process, and the response of pathogens to the catalysis at bio-molecular level. The exploration of the disinfection mechanisms will serve as a guidance to the design of photocatalysts for their large-scale industrial applications.

The disinfection mechanisms of different photocatalysts can be categorized into three aspects: physical damage to the cells by sharp edges of two-dimensional nano structural photocatalysts, toxicity of metal ions released from metal-containing photocatalysts, chemical oxidation of reactive oxidative species (ROSs) and holes produced by photocatalysts. It is recognized that ROSs and holes generated from the photocatalytic process are primarily responsible for the disinfection property, especially against bacteria. As shown in Fig. 11, a schematic diagram of the mechanism of disinfection of bacteria is presented. The photocatalytic disinfection mainly relies on the photoexcitation of a semiconductor by the incident photons with the energy larger than its band gap energy level. In the photocatalytic disinfection process, electrons in the valence band (VB) get excited and move to the conduction band (CB), and photogenerated holes were left in the VB. Finally, photogenerated holes and electrons pairs are involved in redox reactions. Various reactive oxygen species (ROS) on the photocatalyst are formed, including  $\cdot\text{OH}$ ,  $\cdot\text{HO}_2$ ,  $\cdot\text{O}_2^-$ , etc. It is recognized that hydroxyl radicals are majorly responsible for the disinfection property, especially against bacteria. Furthermore, other ROS species can attack the cell wall and cellular components, causing the oxidation of cellular components and membrane leakage (Ref 101). Either of these species attacks the phospholipid membrane of the cell wall and also the oxidation/reduction of the intracellular Co enzyme A, causing cell death and reduction in microbial population. Recently, enormous efforts have been made to study the photocatalytic disinfection mechanism and develop new photocatalysts, in order to acquire high efficiency in disinfection approaches for a wide range of pathogens, including bacteria, viruses, fungi, etc.

**Table 1** Summary of thermal-sprayed photocatalytic materials for biocidal applications

Different strategies	Materials	Microbe	Operation condition		Inactivation efficiency		References
			Microbe level, CFU/mL	Light source	Time, min	Reduction	
Visible-light-induced photocatalysis	TiO <sub>2</sub> coating	<i>E. coli</i>	10 <sup>7</sup> -10 <sup>8</sup>	Solar light	70	4-log	Ref 80
	TiO <sub>2</sub> -Cu coating	<i>P. aeruginosa</i>	10 <sup>4</sup>	Fluorescent lamp	180	75%	Ref 82
	TiO <sub>2</sub> -SrCO <sub>3</sub> coating	<i>E. coli</i>	5 × 10 <sup>7</sup>	Xe lamp	240	99.7%	Ref 83
Black TiO <sub>2</sub>	Black TiO <sub>2</sub> powder	<i>M. aeruginosa</i>	3 × 10 <sup>6</sup>	Xe lamp	720	99.09%	Ref 88
Porous photocatalytic coating	TiO <sub>2</sub> coating	<i>Chlorella</i>	1.8 × 10 <sup>6</sup>	UV lamp	240	70.7%	Ref 98
		<i>P. micans</i>	4.7 × 10 <sup>4</sup>		240	98.6%	
	TiO <sub>2</sub> coating	<i>aeruginosa</i>	10 <sup>4</sup> -10 <sup>8</sup>	UV lamp	5	> 90%	Ref 99
		<i>S. aureus</i>	10 <sup>4</sup> -10 <sup>8</sup>		5-7	> 90%	
<i>C. albicans</i>		10 <sup>3</sup> -10 <sup>5</sup>		30	> 90%		
Recruit and kill strategy	TiO <sub>2</sub> -HA-rGO coating	<i>E. coli</i>	5 × 10 <sup>6</sup>	UV lamp	60	95%	Ref 100
	TiO <sub>2</sub> -Hβ Zeolite powder	<i>E. coli</i>	10 <sup>7</sup>	UV lamp	20	99%	Ref 101
	TiO <sub>2</sub> -HA powder	<i>E. coli</i>	5 × 10 <sup>7</sup>	UV lamp	300	99%	Ref 104, 105
Hollow structured photocatalysts	TiO <sub>2</sub> -Fe <sub>3</sub> O <sub>4</sub> microspheres	<i>E. coli</i>	5 × 10 <sup>7</sup>	UV lamp	300	99%	Ref 107, 108
Self-cleaning photocatalytic coatings	ZnO coating	<i>S. aureus</i>	10 <sup>8</sup>	Simulated sunlight	120	99.5%	Ref 115
Anti-biofilm Topographies	TiO <sub>2</sub> coating	<i>P. aeruginosa</i>	4.7 × 10 <sup>6</sup>	White light	120	24%	Ref 118
	ZnO coating	<i>E. coli</i>	5 × 10 <sup>7</sup>	Sunlight	20	> 99%	Ref 123

**Fig. 11** The possible mechanisms of the photocatalytic disinfection of bacteria (Ref 101)

## Photocatalytic Anti-bacteria Mechanisms

Photocatalytic antibacterial properties are largely related to the bacterial structure. Schematic view of the difference in the antibacterial mechanisms for gram-positive and gram-negative bacteria is illustrated in Fig. 12 (Ref 124). Most bacteria can be classified as gram-positive and gram-negative groups. Their cell walls are made of a complex assembly of high molecular compounds (e.g., peptidoglycan polymers, teichoic acids, lipopolysaccharides, lipoproteins, phospholipids), which are the first surface target of photocatalysis. The outer membrane is absent for the gram-positive bacteria, and the peptidoglycan content of the two is different. Therefore, the primary targets of the gram-positive and gram-negative bacteria may vary, leading to different disinfection mechanisms for the two types of bacteria, where ROSs species with higher oxidation power and concentration are required for the inactivation of gram-positive bacteria because of the multilayered peptidoglycan. On the other hand, the damage effects caused by photocatalysis, including leakage of minerals, genetic material in the microbes, and peroxidation of lipids are common for both the bacteria. Therefore, the photocatalytic disinfections have broad-spectrum antibacterial property.

Among all kinds of microbes, bacteria are identified as an effective indicator for water pollution. *E. coli* is mostly studied among various bacteria and recognized as an indicator for water quality, since its presence generally reflects fecal contamination of water. Extensive studies have been carried out to evaluate various photocatalytic materials that are effective in disinfecting *E. coli*. The

disinfection performances of  $\text{TiO}_2$  photocatalysis have been widely studied over the last two decades. To overcome the shortcomings of  $\text{TiO}_2$ -based photocatalysts, recent research has been pertained to enhancing their photocatalytic inactivation efficiency.

Modification of crystal structure or doping of metals can be used to increase the photocatalytic efficiency by inhibiting photogenerated electron-hole recombination, or increasing visible-light absorption by forming impurity bands. For instance, Zheng et al. developed a one-dimensional photocatalyst from  $\text{Cu-TiO}_2$  nanofibers, it has the advantages of high aspect ratio, large surface area, and limited aggregation (Ref 125, 126). Characterization of the photocatalyst demonstrated that  $\text{Cu}^{2+}$  substituted  $\text{Ti}^{4+}$  in the  $\text{TiO}_2$  lattice and formed an impurity energy level below the conduction band of  $\text{TiO}_2$ , which enabled the nanofibers to realize visible-light response. According to Song et al., the surface modification of rutile phase nano  $\text{TiO}_2$  exhibited two times larger efficiency in *E. coli* disinfection than the unmodified material (Ref 127). Furthermore, it has also been shown that metal doping could enhance photocatalytic efficiency by formatting intermediate bands.

To further investigate the photocatalytic antibacterial mechanisms, Ji et al. studied the disinfection mechanism of a composite nanomaterial of  $\text{Bi}_2\text{WO}_6/\text{TiO}_2/\text{rGO}$ , by using *E. coli* as an indicator (Ref 52). Four scavengers, namely t-BuOH, AO, BQ, and Cr(VI), can be used to scavenge the radical species of  $\text{h}^+$ ,  $\cdot\text{OH}$ ,  $\text{e}^-$ , and  $\cdot\text{O}^{2-}$ , respectively. By intentionally adding different scavengers for comparison examination, the researchers claimed that the photoinduced  $\text{h}^+$  played a vital role in the disinfection process, while  $\cdot\text{OH}$ ,  $\text{e}^-$ , and  $\cdot\text{O}^{2-}$  exhibited synergistic effects.

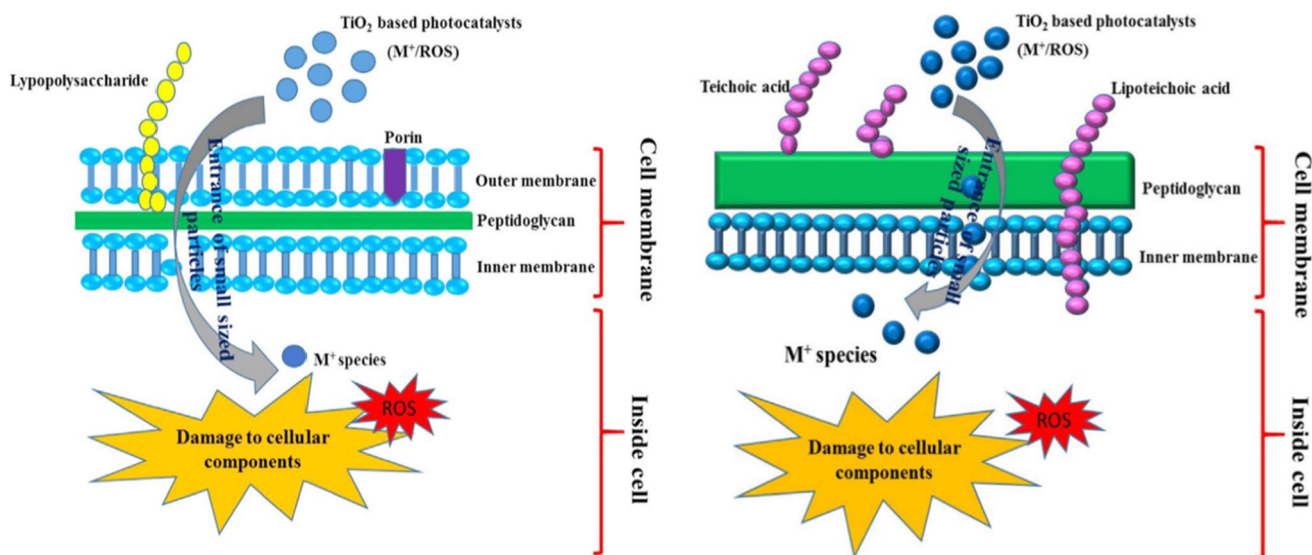


**Fig. 12** Differences in membrane structural composition and proposed antibacterial mechanism for the gram-negative bacteria (left) and the gram-positive bacteria (right) (Ref 124)

### Photocatalytic Anti-virus Mechanisms

There is a vast variety of viruses, which show a different resistance to inactivation in photocatalysis due to different sizes, shapes, structures or compositions. As shown in Fig. 13, the viruses can be classified into two categories, RNA-type and DNA-type viruses, which usually consist of genetic gene (RNA or DNA) and protein shell (capsid). Viral inactivation is mainly related to physical damage, metal toxicity, or ROS species (e.g.,  $\cdot\text{OH}$ ). It must be noted that, unlike the anti-bacteria process, viral disinfection involves denaturation of the rigid protein shell, requiring much more oxidizing power. Based on the current research in the field of photocatalytic viral disinfection, the inactivation falls into three steps: (1) particle shape distortion, (2) protein oxidation, and (3) gene leakage or damage. According to Ishiguro et al., RNA phage Q $\beta$  and DNA phage T4 exhibited a different resistance in a TiO<sub>2</sub>-UV system, where the inactivation of Q $\beta$  was more rapid than that of T4, suggesting the virus gene type influences photocatalytic inactivation kinetics (Ref 128).

The physical damage effect can be evidenced by the comparison study on the viral inactivation ability of graphene oxide (GO) and GO-aptamer-based photocatalysts. Physical damage in viral disinfection is typically involved in graphene-based photocatalysis, for which graphene with many sharp edges cut through protein shells of viruses and inactivated them. It was noted that the bare GO exhibited a similar viricidal activity in dark as that in light (Ref 56). As a comparison, the GO-aptamer with blunt edges posed less viral inactivation than that of the bare GO with sharp edges, confirming that sharp edges of GO played an important role for inactivating viruses physically.

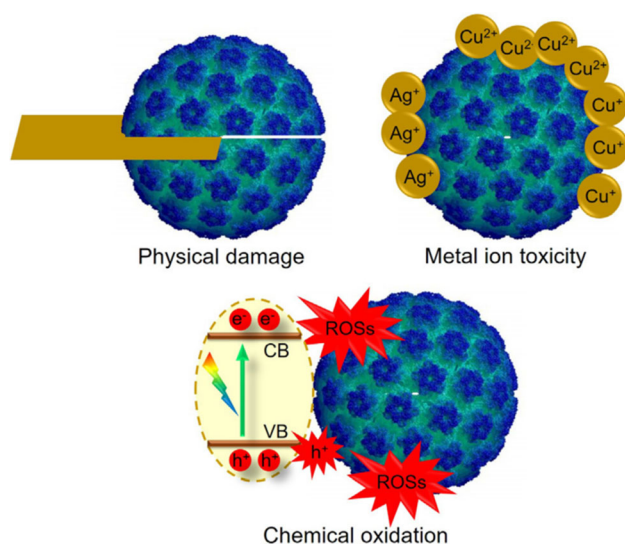


**Fig. 13** Three major mechanisms of viral disinfection induced by photocatalysts (Ref 20)

Considering the metal toxicity, it was revealed that combination of photocatalysis and toxicity of metal ions works synergistically to enhance the disinfection effect. Ditta et al. reported that TiO<sub>2</sub>/CuO films showed faster viral inactivation kinetics than undoped films, although low photoactivity was observed, confirming a major antibacterial and antiviral contribution of released toxic Cu ions (Ref 129). In contrast, there is little to no viral inactivation in the solution containing Ag<sup>+</sup>, of which the concentration was equivalent to that released from Ag/TiO<sub>2</sub> under UV irradiation, suggesting a minor viral disinfection contribution of Ag<sup>+</sup> (Ref 130).

As to the ROS factors, according to the investigation conducted by Zhang (Ref 131), although the estimated concentration of  $\cdot\text{OH}$  was several orders of magnitude lower than that of  $\cdot\text{O}^{2-}$  in g-C<sub>3</sub>N<sub>4</sub>-based disinfection system,  $\cdot\text{OH}$  is still believed to play a critical role in viral inactivation with higher oxidizing power. Hence,  $\cdot\text{OH}$  with a more positive reduction potential than  $\cdot\text{O}^{2-}$  could enable the denaturation process. Furthermore, Horovitz et al. found the difficulty in inactivation of the tested microorganisms is in the order  $E. coli < MS_2 < Aspergillus niger$  (Ref 132). The photocatalytic disinfection testing indicates that the viruses (*MS<sub>2</sub> phage*) were inactivated mainly by the free hydroxyl radicals in the solution, while *E. coli* is inactivated by both the free and the surface-bound hydroxyl radicals and other ROS, such as O<sub>2</sub> and H<sub>2</sub>O<sub>2</sub>.

### Photocatalytic Anti-fungi Mechanisms

The occurrences of pathogenic fungi in daily use water arose increased attention, which posed a potential threat to human health and agriculture production. A couple of published works studied the photocatalytic activity of TiO<sub>2</sub> on disinfection of fungi. The denaturation of the cell wall of fungi is a major aspect for its disinfection. It is believed that the rigid cell wall of fungus acts as a major obstacle, which requires ROSs with high oxidizing power (e.g.,  $\cdot\text{OH}$ ). As illustrated in Fig. 14, the nanoparticle generates hydroxyl radicals ( $\cdot\text{OH}$ ) under visible-light illumination, which directly apply to the surface of fungal cell wall. This radical reacts with glucan and chitin layers of fungal cell wall that results in cell wall degradation and subsequent cell death.

Disinfection of fungi by TiO<sub>2</sub>-based nanomaterials has been reported. Zhang et al. developed a novel method for synthesis of TiO<sub>2</sub> photocatalyst with copper modification and Ti<sup>3+</sup>-doping, and it exhibited broad-spectrum antifungal performances (Ref 133). The work also revealed that the damage of spore walls/membranes of the fungal spores was increased by the photocatalysis, suggesting photo-disinfection mechanism. In another study, disinfection of *Fusarium oxysporum* fungal was realized by TiO<sub>2</sub>

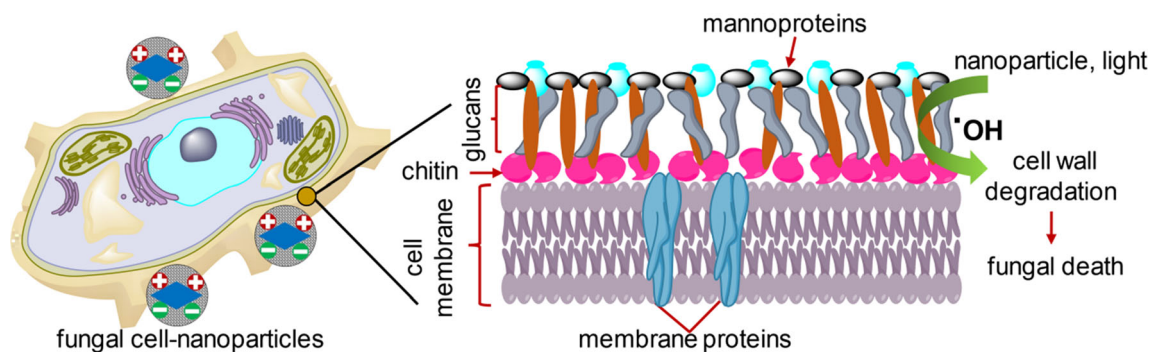


**Fig. 14** Proposed mechanism of antifungal activity of N, F co-doped TiO<sub>2</sub> nanoparticle (Ref 124)

nanoparticles co-doped with N and F exposed under visible light. El-Sayyad et al. reported a gamma-irradiated nanocomposite Co<sub>x</sub>Ni<sub>1-x</sub>Fe<sub>2</sub>O<sub>4</sub>/SiO<sub>2</sub>/TiO<sub>2</sub>  $x = 0.9$  which shows promising antifungal abilities (Ref 134). All these works showed efficient interaction of photocatalytic nanoparticles with the fungal cell wall and visible-light-induced ROS products give rise to the fungal disinfection.

## Conclusions and Future Perspectives

Aimed at the emerging demands for disinfection of pathogenic microbes, many photocatalytic materials have been developed by using different processing routes recently. In this critical review, we have summarized the research works about the typical photocatalytic materials, their biocidal performance, and mechanisms. The thermal spray technique, as a most promising way in fabricating large-scale photocatalytic coatings, has also been reviewed in different trends. Tremendous achievements have been accomplished in this field during the past years, yet it should be pointed out that there still remain a number of challenges, while some of the problems still need to be tackled for further study.

The large-scale preparation and the immobilization of nanomaterial photocatalysts are two key problems for practical applications. Among various surface modification routes, thermal spray method perfectly solves the above problems due to offering a facile one-step fabrication route in realizing large-scale photocatalytic coatings and synthesizing immobilized photocatalytic coatings on desirable solid surfaces for practical use. Through element doping, structure construction, and chemical synthesis during the spraying process, a number of photocatalytic disinfection purposes can be realized by using thermal spray method, including visible-light-induced sterilization, self-cleaning anti-biofouling surface, etc. Black TiO<sub>2</sub> and porous structured antimicrobial photocatalytic coatings are realized by using thermal spray methods to enhance the efficiency in disinfection. Recruitment and killing strategies are realized

by employing thermal spraying and seeking answers in nature.

All in all, thermal spraying method perfectly integrated the novel structural and functional properties in fabricating photocatalytic coatings. However, though a number of studies about the antibacterial application of thermal-sprayed coating were launched, the studies of thermal-sprayed photocatalytic materials and related disinfection mechanisms for anti-virus and anti-fungus applications are still rare. Development of new wide-spectrum and high efficiency photocatalytic materials, theoretical data and inactive mechanisms, and expanding applications for antiviral and anti-fungi purposes still need to explore. With ever-increasing number of scientists focused on this area, we believe that the goals in enhancing the performance and exploring practical use in versatile environments can be achieved in the future.

**Acknowledgments** This research was supported by National Natural Science Foundation of China (Grant # 52071329), Zhejiang Provincial Natural Science Foundation of China (Grant # LY18C100003), the Youth Innovation Promotion Association of the Chinese Academy of Sciences, China (Grant # 2020299), and Innovation 2025 Major Special Programme of Ningbo, China.

## References

1. J. Kaur, R. Karthikeyan, and R. Smith, Assessment of *Escherichia coli* Reactivation After Photocatalytic Water Disinfection Using Flow Cytometry: Comparison with a Culture-Based Method, *Water Sci. Technol. Water Supply*, 2013, **13**(3), p 816-825
2. S. Saran, P. Arunkumar, and S.P. Devipriya, Disinfection of Roof Harvested Rainwater for Potable Purpose Using Pilot-Scale Solar Photocatalytic Fixed Bed Tubular Reactor, *Water Sci Technol Water Supply*, 2018, **18**(1), p 49-59
3. J.H. Castillo-Ledezma, J.L.S. Salas, A. Lopez-Malo, and E.R. Bandala, Effect of pH, Solar Irradiation, and Semiconductor Concentration on the Photocatalytic Disinfection of *Escherichia coli* in Water Using Nitrogen-Doped TiO<sub>2</sub>, *Eur. Food Res. Technol.*, 2011, **233**(5), p 825-834

4. K. Pietrzak and B. Gutarowska, The Effectiveness of Photocatalytic Ionisation Disinfection of Filter Materials, *Pol. J. Microbiol.*, 2013, **62**(2), p 131-139
5. A.Y. Booshehri, R. Wang, and R. Xu, Fabrication of a Catalytic Polymer Composite Sheet Enabling Visible Light-Driven Photocatalytic Disinfection of Water, *Res. Chem. Intermed.*, 2016, **42**(5), p 4827-4838
6. A. Iftikhar, M.S. Khan, U. Rashid, Q. Mahmood, H. Zafar, M. Bilal, and N. Riaz, Influence of Metallic Species for Efficient Photocatalytic Water Disinfection: Bactericidal Mechanism of In Vitro Results Using Docking Simulation, *Environ. Sci. Pollut. Res.*, 2020, <https://doi.org/10.1007/s11356-020-08974-z>
7. H.T. Yu, S. Chen, X. Quan, and Z.H. Zhang, The Mechanism, Materials and Reactors of Photocatalytic Disinfection in Water and Wastewater Treatment, *Prog. Chem.*, 2017, **29**(9), p 1030-1041
8. P. Murugesan, J.A. Moses, and C. Anandharamakrishnan, Photocatalytic Disinfection Efficiency of 2D Structure Graphitic Carbon Nitride-Based Nanocomposites: A Review, *J. Mater. Sci.*, 2019, **54**(19), p 12206-12235
9. J. Gamage and Z.S. Zhang, Applications of Photocatalytic Disinfection, *Int. J. Photoenergy*, 2010, **2010**, p 764870-764880
10. K. Watson, G. Shaw, F.D.L. Leusch, and N.L. Knight, Chlorine Disinfection by-Products in Wastewater Effluent: Bioassay-Based Assessment of Toxicological Impact, *Water Res.*, 2012, **46**(18), p 6069-6083
11. R.E. Selleck, B.M. Saunier, and H.F. Collins, Kinetics of Bacterial Deactivation with Chlorine, *J. Environ. Eng. ASCE*, 1978, **104**(6), p 1197-1212
12. C.A. Castro, A. Jurado, D. Sissa, and S.A. Giraldo, Performance of Ag-TiO<sub>2</sub> Photocatalysts Towards the Photocatalytic Disinfection of Water Under Interior-Lighting and Solar-Simulated Light Irradiations, *Int. J. Photoenergy*, 2012, **2012**, p 261045-261055
13. A. Kubacka, M. Ferrer, and M. Fernandez-Garcia, Kinetics of Photocatalytic Disinfection in TiO<sub>2</sub>-Containing Polymer Thin films: UV and Visible Light Performances, *Appl. Catal. B Environ.*, 2012, **121**, p 230-238
14. N. Kaneva, I. Stambolova, V. Blaskov, Y. Dimitriev, A. Bojinova, and C. Dushkin, A Comparative Study on the Photocatalytic Efficiency of ZnO Thin Films Prepared by Spray Pyrolysis and Sol-Gel Method, *Surf. Coat. Technol.*, 2012, **207**, p 5-10
15. Y.M. Hunge, M.A. Mahadik, V.S. Mohite, S.S. Kumbhar, N.G. Deshpande, K.Y. Rajpure, A.V. Moholkar, P.S. Patil, and C.H. Bhosale, Photoelectrocatalytic Degradation of Methyl Blue Using Sprayed WO<sub>3</sub> Thin Films, *J. Mater. Sci. Mater. Electron.*, 2016, **27**(2), p 1629-1635
16. C. Zhang, Y. Li, D. Shuai, Y. Shen, W. Xiong, and L. Wang, Graphitic Carbon Nitride (g-C<sub>3</sub>N<sub>4</sub>)-Based Photocatalysts for Water Disinfection and Microbial Control: A Review, *Chemosphere*, 2019, **214**, p 462-479
17. B. Reti, Z. Major, D. Szarka, T. Boldizsar, E. Horvath, A. Magrez, L. Forro, A. Dombi, and K. Hernadi, Influence of TiO<sub>2</sub> Phase Composition on the Photocatalytic Activity of TiO<sub>2</sub>/MWCNT Composites Prepared by Combined Sol-Gel/Hydrothermal METHOD, *J. Mol. Catal. A Chem.*, 2016, **414**, p 140-147
18. M. Khraisheh, L.J. Wu, A.H. Al-Muhtaseb, and M.A. Al-Ghouti, Photocatalytic Disinfection of *Escherichia coli* Using TiO<sub>2</sub> P25 and Cu-Doped TiO<sub>2</sub>, *J. Ind. Eng. Chem.*, 2015, **28**, p 369-376
19. C. Sordo, R. Van Grieken, J. Marugan, and P. Fernandez-Ibanez, Solar Photocatalytic Disinfection with Immobilised TiO<sub>2</sub> at Pilot-Plant Scale, *Water Sci. Technol.*, 2010, **61**(2), p 507-512
20. C. Zhang, Y. Li, D.M. Shuai, Y. Shen, and D.W. Wang, Progress and Challenges in Photocatalytic Disinfection of Waterborne Viruses: A Review to Fill Current Knowledge Gaps, *Chem. Eng. J.*, 2019, **355**, p 399-415
21. M. Zhai, Y. Liu, J. Huang, Y. Wang, K. Chen, Y. Fu, and H. Li, Efficient Suspension Plasma Spray fabrication of Black titanium Dioxide Coatings with Visible Light Absorption Performances, *Ceram. Int.*, 2019, **45**(1), p 930-935
22. C. Karunakaran, A. Vijayabalan, G. Manikandan, and P. Gomathisankar, Visible Light Photocatalytic Disinfection of Bacteria by Cd-TiO<sub>2</sub>, *Catal. Commun.*, 2011, **12**(9), p 826-829
23. Y.C. Yan, X.Q. Zhou, J.R. Lan, Z.F. Li, T.L. Zheng, W.B. Cao, N. Zhu, and W.X. Liu, Efficient Photocatalytic Disinfection of *Escherichia coli* by N-Doped TiO<sub>2</sub> Coated on Coal Fly Ash Cenospheres, *J. Photochem. Photobiol. A*, 2018, **367**, p 355-364
24. C. Pablos, J. Marugan, R. van Grieken, P.S.M. Dunlop, J.W.J. Hamilton, D.D. Dionysiou, and J.A. Byrne, Electrochemical Enhancement of Photocatalytic Disinfection on Aligned TiO<sub>2</sub> and Nitrogen Doped TiO<sub>2</sub> Nanotubes, *Molecules*, 2017, **22**(5), p 1-15
25. L. Liu, Z.Y. Liu, H.W. Bai, and D.D. Sun, Concurrent Filtration and Solar Photocatalytic Disinfection/Degradation Using High-Performance Ag/TiO<sub>2</sub> Nanofiber Membrane, *Water Res.*, 2012, **46**(4), p 1101-1112
26. Y. Shimizu, M. Ateia, M.N. Wang, D. Awfa, and C. Yoshimura, Disinfection Mechanism of *E. coli* by CNT-TiO<sub>2</sub> Composites: Photocatalytic Inactivation vs. Physical Separation, *Chemosphere*, 2019, **235**, p 1041-1049
27. M. Long, G. Zhan, M.Y. Sun, H. Zhuang, and R. Wang, Physical Properties of Fe<sup>3+</sup>/TiO<sub>2</sub> Nanoparticles and Photocatalytic Disinfection of Foodborne Microorganisms, *Curr. Top. Nutraceut. Res.*, 2019, **17**(3), p 312-321
28. C. Berberidou, G.Z. Kyzas, I. Paspaltsis, T. Sklaviadis, and I. Poullos, Photocatalytic Disinfection and Purification of Water Employing Reduced Graphene Oxide/TiO<sub>2</sub> Composites, *J. Chem. Technol. Biotechnol.*, 2019, **94**(12), p 3905-3914
29. H. Younas, I.A. Qazi, I. Hashmi, M.A. Awan, A. Mahmood, and H.A. Qayyum, Visible Light Photocatalytic Water Disinfection and Its Kinetics Using Ag-Doped Titania Nanoparticles, *Environ. Sci. Pollut. Res.*, 2014, **21**(1), p 740-752
30. G. Pedroza-Herrera, I.E. Medina-Ramirez, J.A. Lozano-Alvarez, and S.E. Rodil, Evaluation of the Photocatalytic Activity of Copper Doped TiO<sub>2</sub> Nanoparticles for the Purification and/or Disinfection of Industrial Effluents, *Catal. Today*, 2020, **341**, p 37-48
31. N. Janpetch, C. Vanichvattanadecha, and R. Rujiravanit, Photocatalytic Disinfection of Water by Bacterial Cellulose/N-F Coded TiO<sub>2</sub> Under Fluorescent Light, *Cellulose*, 2015, **22**(5), p 3321-3335
32. L.L. Lai and J.M. Wu, A Facile Solution Approach to W, N Coded TiO<sub>2</sub> Nanobelt Thin Films with High Photocatalytic Activity, *J. Mater. Chem. A*, 2015, **3**(31), p 15863-15868
33. R. Leary and A. Westwood, Carbonaceous Nanomaterials for the Enhancement of TiO<sub>2</sub> Photocatalysis, *Carbon*, 2011, **49**(3), p 741-772
34. Y. Fu, Y. Liu, and H. Li, Onion-Like Carbon-Modified TiO<sub>2</sub> Coating by Suspension Plasma Spray with Enhanced PHOTOCATALYTIC Performances, *J. Nanopart. Res.*, 2019, **21**(8), p 1-12
35. O. Akhavan, M. Mehrabian, K. Mirabbaszadeh, and R. Azimrad, Hydrothermal Synthesis of ZnO Nanorod Arrays for Photocatalytic Inactivation of Bacteria, *J. Phys. D Appl.*, 2009, **42**(22), p 225305-225314
36. W. Jiang, T. Huang Fu, X. Yang, L. Bao, Y. Liu, G. Xu, and G. Han, Surfactant-Free Hydrothermal Synthesis of Hierarchical Flower-Like Bi<sub>2</sub>WO<sub>6</sub> Mesosphere Nanostructures with Excellent Visible-Light Photocatalytic Activity, *CrystEngComm*, 2019, **21**(41), p 6293-6300

37. Y.M. Hunge, Sunlight Assisted Photoelectrocatalytic Degradation of Benzoic Acid Using Stratified WO<sub>3</sub>/TiO<sub>2</sub> Thin Films, *Ceram. Int.*, 2017, **43**(13), p 10089-10096
38. T. Yan, J. Huang, J. Bi, L. Xie, and H. Huang, Preparation of Ga<sub>0.25</sub>Zn<sub>4.67</sub>S<sub>5.08</sub> Microsphere by Ultrasonic Spray Pyrolysis and Its Photocatalytic Disinfection Performance Under Visible Light, *J. Nanomater.*, 2019, **2019**, p 9151979
39. S. Wojtyła, W. Macyk, and T. Baran, Photosensitization of CuI—The Role of Visible Light Induced Cu-I, -> Cu-II, Transition in Photocatalytic Degradation of Organic Pollutants and Inactivation of Microorganisms, *Photochem. Photobiol. Sci.*, 2017, **16**(7), p 1079-1087
40. R.M. Trommer, A.K. Alves, and C.P. Bergmann, Synthesis, Characterization and Photocatalytic Property of Flame Sprayed Zinc Oxide Nanoparticles, *J. Alloys Compd.*, 2010, **491**, p 296-300
41. J. Alarcón, S. Ponce, F. Paraguay-Delgado, and J. Rodríguez, Effect of Gamma-Irradiation on the Growth of ZnO Nanorod Films for Photocatalytic Disinfection of Contaminated Water, *J. Colloids Interface Sci.*, 2011, **364**(1), p 49-55
42. L. Sanchez, L. Guz, P. Garcia, S. Ponce, S. Goyanes, M.C. Marchi, R. Candal, W. Estrada, and J. Rodriguez, Influence of Pyrolytic Seeds on ZnO Nanorod Growth onto Rigid Substrates for Photocatalytic Abatement of *Escherichia coli* in Water, *Water Sci. Technol. Water Supply*, 2014, **14**(6), p 1087-1094
43. L. Sanchez, L. Guz, P. Garcia, S. Ponce, S. Goyanes, M. Claudia Marchi, R. Candal, and J. Rodríguez, Synthesis and Characterization of ZnO Nanorod Films on PET for Photocatalytic Disinfection of Water, *J. Adv. Oxid. Technol.*, 2015, **18**(2), p 246-252
44. B. Najma, A.K. Kasi, J.K. Kasi, A. Akbar, S.M.A. Bokhari, and I.R.C. Stroe, ZnO/AAO Photocatalytic Membranes for Efficient Water Disinfection: Synthesis, Characterization and Antibacterial Assay, *Appl. Surf. Sci.*, 2018, **448**, p 104-114
45. A.J. Misra, S. Das, A.P.H. Rahman, B. Das, R. Jayabalan, S.K. Behera, M. Suar, A.J. Tamhankar, A. Mishra, C.S. Lundborg, and S.K. Tripathy, Doped ZnO Nanoparticles Impregnated on Kaolinite (Clay): A Reusable Nanocomposite for Photocatalytic Disinfection of Multidrug Resistant *Enterobacter* sp. Under Visible Light, *J. Colloids Interface Sci.*, 2018, **530**, p 610-623
46. Z.Z. Li, X.C. Meng, and Z.S. Zhang, Hexagonal SnS Nanoplates Assembled onto Hierarchical Bi<sub>2</sub>WO<sub>6</sub> with Enhanced Photocatalytic Activity in Detoxification and Disinfection, *J. Colloids Interface Sci.*, 2019, **537**, p 345-357
47. Z.O. Alarif, M. Anjum, M.O. Ansari, R. Kumar, J. Rashid, M. Madkour, and M.A. Barakat, Synthesis and Characterization of S-Doped-rGO/ZnS Nanocomposite for the Photocatalytic Degradation of 2-Chlorophenol and Disinfection of Real Dairy Wastewater, *J. Photochem. Photobiol. A*, 2019, **377**, p 190-197
48. P. Chandran, P. Kumari, and S.S. Khan, Photocatalytic Activation of CdS NPs Under Visible Light for Environmental Cleanup and Disinfection, *Sol. Energy*, 2014, **105**, p 542-547
49. K. Takehara, K. Yamazaki, M. Miyazaki, Y. Yamada, S. Ruenphet, A. Jahangir, D. Shoham, M. Okamura, and M. Nakamura, Inactivation of Avian Influenza Virus HIM by Photocatalyst Under Visible Light Irradiation, *Virus Res.*, 2010, **151**(1), p 102-103
50. O. Akhavan, M. Choobtashani, and E. Ghaderi, Protein Degradation and RNA Efflux of Viruses Photocatalyzed by Graphene-Tungsten Oxide Composite Under Visible Light Irradiation, *J. Phys. Chem. C*, 2012, **116**(17), p 9653-9659
51. Y.N. Jia, S.H. Zhan, S.L. Ma, and Q.X. Zhou, Fabrication of TiO<sub>2</sub>-Bi<sub>2</sub>WO<sub>6</sub> Binasheet for Enhanced Solar Photocatalytic Disinfection of *E. coli*: Insights on the Mechanism, *ACS Appl. Mater. Interfaces*, 2016, **8**(11), p 6841-6851
52. L. Ji, B. Liu, Y. Qian, Q. Yang, and P. Gao, Enhanced Visible-Light-Induced Photocatalytic Disinfection of *Escherichia coli* by Ternary Bi<sub>2</sub>WO<sub>6</sub>/TiO<sub>2</sub>/Reduced Graphene Oxide Composite Materials: Insight into the Underlying Mechanism, *Adv. Powder Technol.*, 2020, **31**(1), p 128-138
53. Y. Li, J. Zhao, G.S. Zhang, L.L. Zhang, S.Y. Ding, E.X. Shang, and X.H. Xia, Visible-Light-Driven Photocatalytic Disinfection Mechanism of Pb-BiFeO<sub>3</sub>/rGO Photocatalyst, *Water Res.*, 2019, **161**(10), p 251-261
54. P. Gao, J.C. Liu, D.D. Sun, and W. Ng, Graphene Oxide-CdS Composite with High Photocatalytic Degradation and Disinfection Activities Under Visible Light Irradiation, *J. Hazard. Mater.*, 2013, **250**, p 412-420
55. X.M. Song, J.M. Wu, L. Meng, and M. Yan, Enhanced Light Response of Titania Nanotube Arrays Sensitized with Pyrite FeS<sub>2</sub>, *J. Am. Chem. Soc.*, 2010, **93**(7), p 2068-2073
56. K.J. Moor and J.H. Kim, Simple Synthetic Method Toward Solid Supported C-60 Visible Light-Activated Photocatalysts, *Environ. Sci. Technol.*, 2014, **48**(5), p 2785-2791
57. J. Lee, Y. Mackeyev, M. Cho, D. Li, J.H. Kim, L.J. Wilson, and P.J.J. Alvarez, Photochemical and Antimicrobial Properties of Novel C-60 Derivatives in Aqueous Systems, *Environ. Sci. Technol.*, 2009, **43**(17), p 6604-6610
58. M. Cho, J. Lee, Y. Mackeyev, L.J. Wilson, P.J.J. Alvarez, J.B. Hughes, and J.H. Kim, Visible Light Sensitized Inactivation of MS-2 Bacteriophage by a Cationic Amine-Functionalized C-60 Derivative, *Environ. Sci. Technol.*, 2010, **44**(17), p 6685-6691
59. J. Lee, Y. Mackeyev, M. Cho, L.J. Wilson, J.H. Kim, and P.J.J. Alvarez, C-60 Aminofullerene Immobilized on Silica as a Visible-Light-Activated Photocatalyst, *Environ. Sci. Technol.*, 2010, **44**(24), p 9488-9495
60. K.J. Moor, D.C. Valle, C. Li, and J.H. Kim, Improving the Visible Light Photoactivity of Supported Fullerene Photocatalysts Through the Use of C-70 Fullerene, *Environ. Sci. Technol.*, 2015, **49**(10), p 6190-6197
61. X.G. Hu, L. Mu, J.P. Wen, and Q.X. Zhou, Covalently Synthesized Graphene Oxide-Aptamer Nanosheets for Efficient Visible-Light Photocatalysis of Nucleic Acids and Proteins of Viruses, *Carbon*, 2012, **50**(8), p 2772-2781
62. C. Zhang, Y. Li, D.M. Shuai, W.L. Zhang, L.H. Niu, L.F. Wang, and H.J. Zhan, Visible-Light-Driven, Water-Surface-Floating Antimicrobials Developed from Graphitic Carbon Nitride and Expanded Perlite for Water Disinfection, *Chemosphere*, 2018, **208**, p 84-92
63. Y. Liu, X.K. Zeng, X.Y. Hu, J. Hu, and X.W. Zhang, Two-Dimensional Nanomaterials for Photocatalytic Water Disinfection: Recent Progress and Future Challenges, *J. Chem. Technol. Biotechnol.*, 2018, **94**(1), p 22-37
64. J. Xu, Z.P. Wang, and Y.F. Zhu, Enhanced Visible-Light-Driven Photocatalytic Disinfection Performance and Organic Pollutant Degradation Activity of Porous g-C<sub>3</sub>N<sub>4</sub> Nanosheets, *ACS Appl. Mater. Interfaces*, 2017, **9**(33), p 27727-27735
65. S. Ma, S. Zhan, Y. Jia, and Q. Zhou, Superior Antibacterial Activity of Fe<sub>3</sub>O<sub>4</sub>-TiO<sub>2</sub> Nanosheets Under Solar Light, *ACS Appl. Mater. Interfaces*, 2015, **7**(39), p 21875-21883
66. G. Wang, Z. Xing, X.K. Zeng, C.P. Feng, D.T. McCarthy, A. Deletic, and X.W. Zhang, Ultrathin Titanium Oxide Nanosheets Film with Memory Bactericidal Activity, *Nanoscale*, 2016, **8**(42), p 18050-18056
67. Q.J. Zhang, C.H. Sun, Y. Zhao, S.Y. Zhou, X.J. Hu, and P. Chen, Low Ag-Doped Titanium Dioxide Nanosheet Films with Outstanding Antimicrobial Property, *Environ. Sci. Technol.*, 2010, **44**(21), p 8270-8275
68. T.M. Chou, S.W. Chan, Y.J. Lin, P.K. Yang, C.C. Liu, Y.J. Lin, J.M. Wu, J.T. Lee, and Z.H. Lin, A Highly Efficient Au-MoS<sub>2</sub>

- Nanocatalyst for Tunable Piezocatalytic and Photocatalytic Water Disinfection, *Nano Energy*, 2019, **57**, p 14-21
69. F.L. Toma, L.M. Berger, D. Jacquet, D. Wicky, I. Villaluenga, Y.R. de Miguel, and J.S. Lindeløv, Comparative Study on the Photocatalytic Behaviour of Titanium Oxide Thermal Sprayed Coatings from Powders and Suspensions, *Surf. Coat. Technol.*, 2009, **203**(15), p 2150-2156
  70. P. Puddu, S. Popa, G. Bolelli, P. Krieg, M.L. Gualtieri, L. Lusvardi, A. Killinger, and R. Gadov, Suspension HVOF Spraying of TiO<sub>2</sub> Using a Liquid-Fueled Torch, *Surf. Coat. Technol.*, 2018, **349**, p 677-694
  71. M. Robotti, S. Dosta, C. Fernández-Rodríguez, M.J. Hernández-Rodríguez, I.G. Cano, E.P. Melián, and J.M. Guilemany, Photocatalytic Abatement of NO<sub>x</sub> by C-TiO<sub>2</sub>/Polymer Composite Coatings Obtained by Low Pressure Cold Gas Spraying, *Appl. Surf. Sci.*, 2016, **362**, p 274-280
  72. L. Zhou, M. Cai, X. Zhang, N. Cui, G. Chen, and G.Y. Zou, In-Situ Nitrogen-Doped Black TiO<sub>2</sub> with Enhanced Visible-Light-Driven Photocatalytic Inactivation of *Microcystis aeruginosa* Cells: Synthesis, Performance and Mechanism, *Appl. Catal. B Environ.*, 2020, **272**(119019), p 1-10
  73. C. Zhang, U. Chaudhary, S. Das, A. Godavarty, and A. Agarwal, Effect of Porosity on Photocatalytic Activity of Plasma-Sprayed TiO<sub>2</sub> Coating, *J. Therm. Spray Technol.*, 2013, **22**(7), p 1193-1200
  74. H. Cui, J. Jiang, W. Gu, C. Sun, D. Wu, T. Yang, and G. Yang, Photocatalytic Inactivation Efficiency of Anatase Nano-TiO<sub>2</sub> Sol on the H<sub>9</sub>N<sub>2</sub> Avian Influenza Virus, *Photochem. Photobiol.*, 2010, **86**(5), p 1135-1139
  75. H. Chen, L. Zhao, Y. Xiang, Y. He, G.W. Song, X.T. Wang, and F. Liang, A novel Zn-TiO<sub>2</sub>/C@SiO<sub>2</sub> Nanoporous Material on Rice Husk for Photocatalytic Applications Under Visible Light, *Desalin. Water Treat.*, 2016, **57**(21), p 9660-9670
  76. N.C. Birben, A. Tomruk, and M. Bekbolet, The role of Visible Light Active TiO<sub>2</sub> Specimens on the Solar Photocatalytic Disinfection of *E. coli*, *Environ. Sci. Pollut. Res.*, 2017, **24**(14), p 12618-12627
  77. T. Koklic, S. Pintaric, I. Zdovc, M. Golob, P. Umek, A. Mehle, M. Dobeic, and J. Strancar, Photocatalytic Disinfection of Surfaces with Copper Doped TiO<sub>2</sub> Nanotube Coatings Illuminated by Ceiling Mounted Fluorescent Light, *PLoS ONE*, 2018, **13**(5), p 1-17
  78. M. Feilizadeh, G. Mul, and M. Vossoughi, *E. coli* Inactivation by Visible Light Irradiation Using a Fe-Cd/TiO<sub>2</sub> Photocatalyst: Statistical Analysis and Optimization of Operating Parameters, *Appl. Catal. B Environ.*, 2015, **168**, p 441-447
  79. L.G. Bettini, M.V. Diamanti, M. Sansotera, M.P. Pedferri, W. Navarrini, and P. Milani, Immobilized TiO<sub>2</sub> Nanoparticles Produced by Flame Spray for Photocatalytic Water Remediation, *J. Nanopart. Res.*, 2016, **18**(8), p 238-247
  80. M. Nararom, S. Thepa, J. Kongkiattikajorn, and R. Songprakorp, Disinfection of Water Containing *Escherichia coli* by Use of a Compound Parabolic Concentrator: Effect of Global Solar Radiation and Reactor Surface Treatment, *Res. Chem. Intermed.*, 2015, **41**(9), p 6543-6558
  81. P. Ctibor, Z. Pala, V. Stengl, and R. Musalek, Photocatalytic Activity of Visible-Light-Active Iron-Doped Coatings Prepared by Plasma Spraying, *Ceram. Int.*, 2014, **40**(1), p 2365-2372
  82. N. George, M. Mahon, and A. McDonald, Bactericidal Performance of Flame-Sprayed Nanostructured Titania-Copper Composite Coatings, *J. Therm. Spray Technol.*, 2010, **19**(5), p 1042-1053
  83. M. Zhai, Y. Liu, J. Huang, W. Hou, S. Wu, B. Zhang, and H. Li, Fabrication of TiO<sub>2</sub>-SrCO<sub>3</sub> Composite Coatings by Suspension Plasma Spraying: Microstructure and Enhanced Visible Light Photocatalytic Performances, *J. Therm. Spray Technol.*, 2020, **29**(5), p 1172-1182
  84. X. Chen, L. Liu, P.Y. Yu, and S.S. Mao, Increasing Solar Absorption for Photocatalysis with Black Hydrogenated Titanium Dioxide Nanocrystals, *Science*, 2011, **331**(6018), p 746-750
  85. C.C. Chen, X.Z. Li, W.H. Ma, J.C. Zhao, H. Hidaka, and N. Serpone, Effect of Transition Metal Ions on the TiO<sub>2</sub>-Assisted Photodegradation of Dyes Under Visible Irradiation: A Probe for the Interfacial Electron Transfer Process and Reaction Mechanism, *J. Phys. Chem. B*, 2002, **106**(2), p 318-324
  86. S.E. Heo, H.W. Lim, D.K. Cho, I.J. Park, H. Kim, C.W. Lee, S.H. Ahn, and J.Y. Kim, Anomalous Potential Dependence of Conducting Property in Black Titania Nanotube Arrays for Electrocatalytic Chlorine Evolution, *J. Catal.*, 2020, **381**, p 462-467
  87. K. Carlson, C. Elliott, S. Walker, M. Misra, and S. Mohanty, An Effective, Point-of-Use Water Disinfection Device Using Immobilized Black TiO<sub>2</sub> Nanotubes as an Electrocatalyst, *J. Electrochem. Soc.*, 2016, **163**(6), p H395-H401
  88. L. Zhou, M. Cai, X. Zhang, N. Cui, G. Chen, and G.Y. Zou, In-Situ Nitrogen-Doped Black TiO<sub>2</sub> with Enhanced Visible-Light-Driven Photocatalytic Inactivation of *Microcystis aeruginosa* Cells: Synthesis, Performance and Mechanism, *Appl. Catal. B Environ.*, 2020, **272**, p 119019-119028
  89. Y. Xu, W. Wen, and J.M. Wu, Titania Nanowires Functionalized Polyester Fabrics with Enhanced Photocatalytic and Antibacterial Performances, *J. Hazard. Mater.*, 2018, **343**, p 285-297
  90. R. Purbia, R. Borah, and S. Paria, Carbon-Doped Mesoporous Anatase TiO<sub>2</sub> Multi-tubes Nanostructures for Highly Improved Visible Light Photocatalytic Activity, *Inorg. Chem.*, 2017, **56**(16), p 10107-10116
  91. J. Yang, X. Zhang, B. Li, H. Liu, P. Sun, C. Wang, L. Wang, and Y. Liu, Photocatalytic Activities of Heterostructured TiO<sub>2</sub>-Graphene Porous Microspheres Prepared by Ultrasonic Spray Pyrolysis, *J. Alloys Compd.*, 2014, **584**, p 180-184
  92. B.W. Robinson, C.J. Tighe, R.I. Gruar, A. Mills, I.P. Parkin, A.K. Tabecki, H.L.D.V. Lovelock, and J.A. Darr, Suspension Plasma Sprayed Coatings Using Dilute Hydrothermally Produced Titania Feedstocks for Photocatalytic Applications, *J. Mater. Chem. A*, 2015, **3**(24), p 12680-12689
  93. O. Sugiyama, M. Okuya, and S. Kaneko, Photocatalytic Ability of TiO<sub>2</sub> Porous Film Prepared by Modified Spray Pyrolysis Deposition Technique, *J. Ceram. Soc. Jpn.*, 2009, **117**(1362), p 203-207
  94. R. Jbeli, A. Boulthachem, F. Saadallah, S. Alleg, M. Amlouk, and H. Ezzaouia, Synthesis and Physical Properties of Fe Doped La<sub>2</sub>O<sub>3</sub> Thin Films Grown by Spray Pyrolysis for Photocatalytic Applications, *Mater. Res. Exp.*, 2019, **6**(6), p 1-10
  95. L. Zhang, S. Yu, K. Wang, J. Zhang, and J. Fang, A Cost- and Time-saving Strategy of Spraying TiO<sub>2</sub> Self-Cleaning Coatings in Tubular Substrates by Air Cold Plasma, *Chem. Phys. Lett.*, 2017, **687**, p 205-208
  96. Y.F. Lin, K.L. Tung, Y.S. Tzeng, J.H. Chen, and K.S. Chang, Rapid Atmospheric Plasma Spray Coating Preparation and Photocatalytic Activity of Macroporous Titania Nanocrystalline Membranes, *J. Membr. Sci.*, 2012, **389**, p 83-90
  97. M.C. Bordes, M. Vicent, R. Moreno, J. Garcia-Montano, A. Serra, and E. Sanchez, Application of Plasma-Sprayed TiO<sub>2</sub> Coatings for Industrial (Tannery) Wastewater Treatment, *Ceram. Int.*, 2015, **41**(10), p 14468-14474
  98. T.H. Kim, S.W. Lee, H. Chen, and H.Y. Cho, Photocatalytic Characterization of Plasma Sprayed TiO<sub>2</sub> Coating in Environmental Engineering Application, *Mater. Sci. Forum*, 2006, **510-511**, p 70-73

99. J.W. Macfarlane, H.F. Jenkinson, and T.B. Scott, Sterilization of Microorganisms on Jet Spray Formed Titanium Dioxide Surfaces, *Appl. Catal. B Environ.*, 2011, **106**(1–2), p 181-185
100. J. Huang, Y. Gong, Y. Liu, X. Suo, and H. Li, Developing Titania-Hydroxyapatite-Reduced Graphene Oxide Nanocomposite Coatings by Liquid Flame Spray Deposition for Photocatalytic Applications, *J. Eur. Ceram. Soc.*, 2017, **37**(12), p 3705-3711
101. M.P. Reddy, H.H. Phil, and M. Subrahmanyam, Photocatalytic Disinfection of *Escherichia coli* over Titanium(IV) Oxide Supported on H Beta Zeolite, *Catal. Lett.*, 2008, **123**, p 56-64
102. M. Giannouri, T. Kalampaliki, N. Todorova, T. Giannakopoulou, N. Boukos, D. Petrakis, T. Vaimakis, and C. Trapalis, One-Step Synthesis of TiO<sub>2</sub>/Perlite Composites by Flame Spray Pyrolysis and Their Photocatalytic Behavior, *Int. J. Photoenergy*, 2013, **2013**, p 729460-729467
103. A. Nakajima, K. Takakuwa, Y. Kameshima, M. Hagiwara, S. Sato, Y. Yamamoto, N. Yoshida, T. Watanabe, and K. Okada, Preparation and Properties of Titania-Apatite Hybrid Films, *J. Photochem. Photobiol. A Chem.*, 2006, **177**(1), p 94-99
104. Y. Liu, J. Huang, S. Ding, Y. Liu, J. Yuan, and H. Li, Deposition, Characterization, and Enhanced Adherence of *Escherichia coli* Bacteria on Flame-Sprayed Photocatalytic Titania-Hydroxyapatite Coatings, *J. Therm. Spray Technol.*, 2013, **22**(6), p 1053-1062
105. J. Huang, Y. Liu, Y. Liu, and H. Li, Hydroxyapatite Nucleated and Grown on Nano Titania Particles Enhances Recruitment of *Escherichia coli* for Subsequent Photocatalytic Elimination, *Mater. Chem. Phys.*, 2015, **151**, p 364-371
106. Y. Yamaguchi, S. Usuki, Y. Kanai, K. Yamatoya, N. Suzuki, K.I. Katsumata, C. Terashima, T. Suzuki, A. Fujishima, H. Sakai, A. Kudo, and K. Nakata, Selective Inactivation of Bacteriophage in the Presence of Bacteria by Use of Ground Rh-Doped SrTiO<sub>3</sub> Photocatalyst and Visible Light, *ACS Appl. Mater. Interfaces*, 2017, **9**(37), p 31393-31400
107. K. Ren, Y. Liu, X. He, and H. Li, Suspension Plasma Spray Fabrication of Nanocrystalline Titania Hollow Microspheres for Photocatalytic Applications, *J. Therm. Spray Technol.*, 2015, **24**(7), p 1213-1220
108. X. He, K. Ren, Y. Liu, J. Huang, and H. Li, Hollow Plasma-Sprayed Spherical Nanostructured Titania Feedstock for Photocatalytic Applications, *J. Therm. Spray Technol.*, 2018, **27**(8), p 1532-1541
109. S. Giannakis, S. Liu, A. Carratala, S. Rtimi, M.T. Amiri, M. Bensimon, and C. Pulgarin, Iron Oxide-Mediated Semiconductor Photocatalysis vs. Heterogeneous Photo-Fenton Treatment of Viruses in Wastewater. Impact of the Oxide Particle Size, *J. Hazard. Mater.*, 2017, **339**, p 223-231
110. W.J. Ma, Y.C. Ding, M.J. Zhang, S.T. Gao, Y.S. Li, C.B. Huang, and G.D. Fu, Nature-Inspired Chemistry Toward Hierarchical Superhydrophobic, Antibacterial and Biocompatible Nanofibrous Membranes for Effective UV-Shielding, Self-Cleaning and Oil-Water Separation, *J. Hazard. Mater.*, 2020, **384**, p 121476-121488
111. J. Yuan, Q. Zhan, Q. Lei, S. Ding, and H. Li, Fabrication and Characterization of Hybrid Micro/Nano-Structured Hydrophilic Titania Coatings Deposited by Suspension Flame Spraying, *Appl. Surf. Sci.*, 2012, **258**(17), p 6672-6678
112. H.Y. He, Photoinduced Superhydrophilicity and High Photocatalytic Activity of ZnO-Reduced Graphene Oxide Nanocomposite Films for Self-Cleaning Applications, *Mater. Sci. Semicond. Proc.*, 2015, **31**, p 200-208
113. Y. Won, K. Schwartzberg, and K.A. Gray, TiO<sub>2</sub>-Based Transparent Coatings Create Self-Cleaning Surfaces, *Chemosphere*, 2018, **208**, p 899-906
114. H. Teisala, M. Tuominen, M. Aromaa, J.M. Makela, M. Stepien, J.J. Saarinen, M. Toivakka, and J. Kuusipalo, Development of Superhydrophobic Coating on Paperboard Surface Using the Liquid Flame Spray, *Surf. Coat. Technol.*, 2010, **205**(2), p 436-445
115. L. Valenzuela, Antimicrobial Surfaces with Self-Cleaning Properties Functionalized by Photocatalytic ZnO Electrospayed Coatings, *J. Hazard. Mater.*, 2019, **369**, p 665-673
116. H.F. Huang, Y.Q. An, X. Hu, D. Wu, H.W. Cao, X. Zhang, J.H. Qiao, and H.T. Liu, A Plasma Sprayed Superhydrophobic Coating Prepared with Al@WO<sub>3</sub> Core-Shell Powder and Photocatalytic Degradation Performance, *Surf. Coat. Technol.*, 2019, **369**, p 105-115
117. M.F. Blanca Jalvoa, A. Bahamonde, and R. Rosal, Antimicrobial and Antibiofilm Efficacy of Self-Cleaning Surfaces Functionalized by TiO<sub>2</sub> Photocatalytic Nanoparticles Against *Staphylococcus aureus* and *Pseudomonas putida*, *J. Hazard. Mater.*, 2017, **340**, p 160-170
118. B. Jeffery, M. Pepler, R.S. Lima, and A. McDonald, Bactericidal Effects of HVOF-Sprayed Nanostructured TiO<sub>2</sub> on *Pseudomonas aeruginosa*, *J. Therm. Spray Technol.*, 2010, **19**, p 344-349
119. Y. Kikuchi, K. Sunada, T. Iyoda, K. Hashimoto, and A. Fujishima, Photocatalytic Bactericidal Effect of TiO<sub>2</sub> Thin Films: Dynamic View of the Active Oxygen Species Responsible for the Effect, *J. Photochem. Photobiol. A Chem.*, 1997, **106**, p 51-56
120. J. Rodríguez, F. Paraguay-Delgado, A. López, J. Alarcón, and W. Estrada, Synthesis and Characterization of ZnO Nanorod Films for Photocatalytic Disinfection of Contaminated Water, *Thin Solid Films*, 2010, **519**, p 729-735
121. K. Chen, Y. Liu, Y. Fu, J. Huang, X. Feng, J. Wang, M. Zhai, R. Lupoi, S. Yin, and H. Li, Loading of Zn/ZnO Particles in the Precursor Feedstock Affects the Characteristics of Liquid Plasma Sprayed Nano-ZnO Coatings for Photocatalytic Applications, *Nanotechnology*, 2020, **31**(18), p 185301
122. S. Heinonen, M. Kannisto, J.P. Nikkanen, E. Huttunen-Saarivirta, M. Karp, and E. Levanen, Photocatalytic and Antibacterial Properties of ZnO Films with Different Surface Topographies on Stainless Steel Substrate, *Thin Solid Films*, 2016, **616**, p 842-849
123. J. Rodríguez Rodríguez, F. Paraguay-Delgado, A. Lopez, J. Alarcon, and W. Estrada, Synthesis and Characterization of ZnO Nanorod Films for Photocatalytic Disinfection of Contaminated Water, *Thin Solid Films*, 2010, **519**(2), p 729-735
124. P. Venkata, L. Reddy, B. Kavith, P. Anil, K. Reddy, and K.H. Kim, TiO<sub>2</sub>-Based Photocatalytic Disinfection of Microbes in Aqueous Media: A Review, *Environ. Res.*, 2017, **154**, p 296-303
125. X. Zheng, Z.P. Shen, C. Cheng, L. Shi, R. Cheng, and J. Dong, Electrospinning Cu-TiO<sub>2</sub> Nanofibers Used for Photocatalytic Disinfection of Bacteriophage f2: Preparation, Optimization and Characterization, *RSC Adv.*, 2017, **7**(82), p 52172-52179
126. X. Zheng, Z.P. Shen, C. Cheng, L. Shi, R. Cheng, and D.H. Yuan, Photocatalytic Disinfection Performance in Virus and Bacteria System by Cu-TiO<sub>2</sub> Nanofibers Under Visible Light, *Environ. Pollut.*, 2018, **237**, p 452-459
127. G.S. Song, C.Z. Luo, Q. Fu, and C.X. Pan, Hydrothermal Synthesis of the Novel Rutile-Mixed Anatase TiO<sub>2</sub> Nanosheets with Dominant 001 Facets for High Photocatalytic Activity, *RSC Adv.*, 2016, **6**(87), p 84035-84041
128. H. Ishiguro, R. Nakano, Y. Yao, J. Kajioaka, A. Fujishima, K. Sunada, M. Minoshima, K. Hashimoto, and Y. Kubota, Photocatalytic Inactivation of Bacteriophages by TiO<sub>2</sub>-Coated Glass Plates Under Low-Intensity, Long-Wavelength UV Irradiation, *Photochem. Photobiol. Sci.*, 2011, **10**(11), p 1825-1829

129. I.B. Ditta, A. Steele, C. Liptrot, J. Tobin, H. Tyler, H.M. Yates, D.W. Sheel, and H.A. Foster, Photocatalytic Antimicrobial Activity of Thin Surface Films of TiO<sub>2</sub>, CuO and TiO<sub>2</sub>/CuO Dual Layers on *Escherichia coli* and Bacteriophage T<sub>4</sub>, *Appl. Microbiol. Biotechnol.*, 2008, **79**(1), p 127-133
130. M.V. Liga, E.L. Bryant, V.L. Colvin, and Q. Li, Virus Inactivation by Silver Doped Titanium Dioxide Nanoparticles for Drinking Water Treatment, *Water Res.*, 2011, **45**(2), p 535-544
131. C. Zhang, Y. Li, W. Zhang, P. Wang, and C. Wang, Metal-Free Virucidal Effects Induced by g-C<sub>3</sub>N<sub>4</sub> Under Visible Light Irradiation: Statistical Analysis and Parameter Optimization, *Chemosphere*, 2018, **195**, p 551-558
132. I. Horovitz, D. Avisar, E. Luster, L. Lozzi, T. Luxbacher, and H. Mamane, MS<sub>2</sub> Bacteriophage Inactivation Using a N-doped TiO<sub>2</sub>-Coated Photocatalytic Membrane Reactor: Influence of Water-Quality Parameters, *Chem. Eng. J.*, 2018, **354**, p 995-1006
133. J. Zhang, M. Yuan, X. Liu, X. Wang, S. Liu, B. Han, B. Liu, and H. Shi, Copper Modified Ti<sup>3+</sup> Self-Doped TiO<sub>2</sub> Photocatalyst for Highly Efficient Photodisinfection of Five agricultural Pathogenic Fungus, *Chem. Eng. J.*, 2020, **387**, p 124171-124179
134. G.S. El-Sayyad, M. Abd Elkodous, A.M. El-Khawaga, M.A. Elsayed, A.I. El-Batal, and M. Gobara, Merits of Photocatalytic and Antimicrobial Applications of Gamma-Irradiated Co<sub>x</sub>Ni<sub>1-x</sub>Fe<sub>2</sub>O<sub>4</sub>/SiO<sub>2</sub>/TiO<sub>2</sub>, x = 0.9 Nanocomposite for Pyridine Removal and Pathogenic Bacteria/Fungi Disinfection: Implication for Wastewater Treatment, *RSC Adv.*, 2020, **10**(9), p 5241-5259

**Publisher's Note** Springer Nature remains neutral with regard to jurisdictional claims in published maps and institutional affiliations.